The analysis of column supported plates with special application to bridges

The Analysis of Column Supported Plates with Special Application to Bridges

Le calcul des dalles appuyées sur piliers, eu égard plus particulièrement aux ponts

Die Analyse säulengestützter Platten mit besonderer Anwendung auf Brücken

L. S. D. MORLEY

Royal Aircraft Establishment Farnborough, Hants.

1. Introduction

The present paper deals with the theoretical analysis of a thin flat plate which is supported by many diversely spaced columns and loaded by concentrated forces normal to its plane. The problem is one of importance because it occurs in so many different engineering contexts. In particular, the current expansion of the road network in Great Britain requires the design of elevated roads with complicated arrangements of columns like that at the Cumberland Basin in Bristol, where the essential structure consists of a reinforced concrete slab which is supported upon diversely spaced columns. Resort has often been made to model tests (see e. g. BEST and WEST [1]) in order to obtain the design data for this type of construction. Such tests provide, however, only the minimum data for the specific project, for it is difficult to optimize the design through modification of the model or to investigate such effects as settlement, change of Poisson's ratio or change in the orthotropy subsequent to cracking of the concrete. Moreover, the time which is consumed during the construction and testing of the model is an important factor in competitive design.

As noted by ANDRÄ and LEONHARDT [2] and RÜSCH and HERGENRÖDER [3], there is a dearth of reliable theoretical results even for the relatively simple problem of the single span skew slab and, in consequence, they make resort to extensive model tests in order to derive tabulations of basic design data. A main difficulty in a theoretical analysis is that the column supported plate presents

a boundary value problem which is complicated by the presence of the statically indeterminate column reactions.

In a theoretical analysis it is simpler, and usually quite reasonable, to replace each column by a concentrated load of such intensity that the deflection of the plate is allowed to take up just the prescribed amount of column settlement whilst undergoing the applied loading condition, it being assumed that the local problems presented by the finite size of the columns can be treated subsequently and separately. It must be borne in mind, however, that this simplification now provides us with a mathematical problem in the classical theory of plate bending where the second and higher derivatives of the deflection are discontinuous at the concentrated load positions (it is recalled that the bending moments depend upon the second derivatives and the shearing forces upon the third derivatives of the deflection). Now, it has been pointed out previously [4] that many approximate methods of solution to boundary value problems in continuum mechanics proceed as if the solution is regular so that their success is related in some measure with the "degree of regularity" of the actual solution, i. e. with the continuity of the successive derivatives of the deflection. It follows, therefore, that it is good practice to make proper allowance in our solution for the discontinuous behaviour which occurs in the second and higher derivatives of the deflection at the concentrated load and column positions. In this connection, it is noted that the finite difference, finite element and grillage methods set out to solve this same basic mathematical problem and, although they provide many valuable results for engineering problems, they usually make no provision for this discontinuous behaviour. These methods require, moreover, a long and continuous sequence of arithmetic operations which can provide opportunity for an accumulation of errors. Furthermore, they predict finite values for the bending moments in the plate at the column positions and underneath concentrated loads and, in view of the discontinuity of the second derivatives of the deflection, these values are dependent upon the size of the mesh. Although these values, obtained in approximation to infinity, are often compared with those obtained experimentally there are obvious difficulties in drawing worthwhile conclusions because the inadequacies of numerical methods provide proper allowance neither for the two dimensional character of the actual load distribution nor for the averaging effect of the particular strain measuring device.

The present analysis employs exact techniques associated with the classical theory of plate bending (see e. g. TIMOSHENKO and WOINOWSKY-KRIEGER [5]) in conjunction with principles which are derived by an engineering appraisal of the problem. For example, in order to reduce the number of sequential arithmetic operations it is expedient to separate, as far as is possible, the calculations for the statically indeterminate column reactions from those which are required for the boundary value problem of the rectangular plate. Thus, the simpler problem of a column supported plate is first considered where the boundary is

extended so that the flat plate becomes of infinite extent. Effective precautions can now be taken e. g. by collecting the column reactions into statically zero force groups, to deal with the sensitivity in calculating the deflections and to deal also with the discontinuities in the solution but without the encumbrance of a boundary value problem. Moreover, this statically indeterminate solution is conveniently expressed in explicit terms after the inversion of a matrix of only the same order as the number of columns. The columns and applied loading are next removed for the solution of the boundary value problem, which now concerns a rectangular plate loaded only at the boundary by a system of self-equilibrating shearing forces and bending moments. To simplify matters still further, the rectangular plate is considered to be of sufficient length so that the behaviour at the column positions is dependent only upon the resultants of the tractions at the ends of the rectangular plate and not upon their manner of distribution. This boundary value problem is solved by straightforward Fourier synthesis of the tractions acting at the long edges and requires the inversion only of second order matrices. The broad outline of an iterative process is now apparent. The statically indeterminate problem is solved for the infinite plate with the prescribed loading and the prescribed column settlements. The "residual" shearing forces and bending moments are then calculated along the lines which correspond with the boundary of the actual rectangular plate. These residuals are now reversed and applied along the boundary of the unrestrained rectangular plate, and the resulting deflections are calculated at each column position. These deflections, in their turn, are regarded as column settlements to be superimposed upon the prescribed settlements for the infinite plate solution. The process is repeated as many times as is required until steady state values are obtained for the column reactions.

These ideas have a wide application but they are confined here, for definiteness, to the rectangular plate which is of constant thickness and is isotropic, although an Appendix provides the basic equations for the orthotropic case. A computer program has been developed in conjunction with the analysis to deal with a quite arbitrary disposition and number of columns, column settlements and loading arrangements. The program provides all the column reactions as well as the bending and twisting moments at any required station. Extensive use is made of matrix operations and the program can be readily adapted to other situations such as where the boundary is reinforced, the plate is orthotropic or the columns are elastic. The question of linear elastic column supports can, alternatively, be dealt with by an auxiliary calculation and an example is given later in the paper.

Problems of plates supported on continuously distributed bearings can often be approximated by column supported plates and comparisons of this kind are provided in the numerical examples which conclude the paper, along with extensive comparisons from model tests on skew slabs and the Cumberland Basin elevated road system. In making these comparisons there has been no

attempt to achieve, or even to investigate, economy in computer usage by restricting the number of iterations or the number of terms in the Fourier synthesis; attention has been confined to achieving an assured high standard of accuracy (usually to within four significant figures). The numerical example for the Cumberland Basin elevated road system shows, however, that the preliminary infinite plate solution can provide a good indication of the peak column reactions for this type of continuous bridge and this then provides a design tool which is extremely economical in computer usage. Economies may be achieved in other ways such as by restricting attention to separate localised areas in a bridge of considerable extent. A general conclusion which arises from the comparisons with the model tests is that it is a matter of some difficulty to conduct these tests in such a way as to obtain reliable results for the column reactions. A main difficulty is that the load measuring devices inevitably possess inherent elastic characteristics and these exert their own influence on the column reactions which are found to be highly sensitive to any kind of settlement, relative or elastic, of the supports. The effect of this settlement is to redistribute the load away from the heavily loaded columns and so to provide optimistic values for the peak reactions. In consequence, the numerical results from the present method are found to provide pessimistic values for the peak reactions in all the comparisons with model tests.

Towards the end of the present investigation the author's attention was drawn to a recent, and remarkable, paper by JEAN-CLAUDE LERAY [6] which gives details of many results obtained from a computer program specially developed for the analysis of column supported plates of infinite length. The analysis is due to JEAN LERAY [7, 8] and proceeds from a numerically determined biharmonic Green's function for an infinitely long strip with free edges and supported at infinity. Although his method takes into proper account the discontinuities of the solution, a sensitivity is indicated by the use of triple length arithmetic (24 significant figures) for part of the calculations. There are also limitations upon the number (40) and precise disposition of the column supports and applied loading.

The author is indebted to Mr. B. C. MERRIFIELD for his assistance with the development of the computer program.

2. Notation

An explanation is given first for the various combinations of suffices and an affix which are used in conjunction with the list of basic notation given at the end of this paragraph.

The analysis commences by gathering the statically indeterminate column reactions into self-equilibrating force groups F_α where the suffix α always denotes relevance to quantities immediately associated with this force group;

the suffix β always denotes similar relevance to quantities immediately associated with the principal force groups F_β for the applied loading.

The solution is obtained through an iterative process, starting from a preliminary infinite plate solution where the various quantities bear the suffix inf, e. g. $w_{inf}(x,y)$, $M_{y,inf}(x,y)$, etc. We then proceed to a boundary value problem for an unrestrained rectangular plate where the various quantities of this intermediate solution bear the affix (F), e. g. $w^{(F)}(x,y)$, $M_y^{(F)}(x,y)$. A return is now made to the infinite plate where this intermediate solution bears both the suffix inf and the affix (F), e. g. $w_{inf}^{(F)}(x,y)$, $M_{y,inf}^{(F)}(x,y)$ etc. The various quantities appropriate to the final solution of the boundary value problem, see Eq. (8.3) et seq, of the column supported plate are denoted simply by $w(x,y)$, $M(x,y)$, etc.

The following list provides the basic notation for the fundamental quantities.

a	length of the rectangular plate, the ends are located at $x = 0, a$.
$2b$	width of the rectangular plate, the sides are located at $y = \pm b$.
A_n, B_n, C_n, D_n	constants which are associated with the nth terms of the Fourier series.
c	constant used in the iteration process, typically $0.1 \leqq c \leqq 1.0$.
C	denotes the boundary of the rectangular plate.
C_l, C_{l-1}, C_{l-2}	constants which account for the rigid body movements of the plate.
$c_{\alpha m}$	used in defining the force group F_α, a positive value corresponds with a column compression.
C_α	the intensity of the force group F_α.
D	flexural rigidity of the plate.
F	a vector quantity which describes all the column reactions.
i, j, k, k', m	integers which refer usually to column numbers.
l	the plate is supported upon l columns.
l'	the number of applied loads.
$M(x)$	resultant bending moment at an end of the rectangular plate.
$M_x(x,y)$, $M_y(x,y)$, $M_{xy}(x,y)$	plate bending and twisting moments of the $x\,0\,y$ co-ordinate system.
n	integer which refers to the nth term of the Fourier series.
N	non-dimensional elasticity parameter for the column supports.

p_m — concentrated load of unit intensity acting downwards at the position $x = x_m$, $y = y_m$.

$Q_x(x, y)$, $Q_y(x, y)$ — shearing forces of the $x\,0\,y$ co-ordinate system.

r — distance from origin of co-ordinates, $r^2 = x^2 + y^2$.

r_i — defined by Eq. (4.8).

r_α — defined by Eq. (4.13).

$r_{\alpha i}$ — defined by Eq. (4.11).

s — distance measured around the boundary of the rectangular plate.

$T(x)$ — resultant twisting moment at an end of the rectangular plate.

$V_x(x, y)$, $V_y(x, y)$ — Kirchhoff normal forces of the $x\,0\,y$ co-ordinate system.

$w(x, y)$ — the normal deflection of the plate.

$w_{col\,set}(x_i, y_i)$ — the prescribed settlement of column i.

x, y — rectangular Cartesian co-ordinates.

x_α, y_α — the co-ordinates of some point which lies within the immediate vicinity of the force group F_α, see Eq. (4.9).

γ_n — $= n\,\pi/a$.

Γ_α — a constant which is associated with the force group F_α, it is defined by Eq. (4.10).

λ' — a constant which is used during the iterative process, see Section 8.

Λ' — provides an indication of the convergence of the iterative process, it is defined by Eq. (8.5).

ν — Poisson's ratio.

ν — the outward normal to the boundary, used only in Section 8.

A few additional symbols are used in Appendix A, they are defined as they are introduced.

3. Fundamental Equations

The fundamental equations are well known but they are listed below for purposes of easy reference.

The plate is assumed to lie in the horizontal plane with rectangular co-ordinate axes $x\,0\,y$ as shown in Fig. 1; the deflection w is positive downwards. The expressions for the bending and twisting moments are

$$M_x = -D \left(\frac{\partial^2 w}{\partial x^2} + \nu \frac{\partial^2 w}{\partial y^2} \right), \tag{3.1 a}$$

$$M_y = -D \left(\frac{\partial^2 w}{\partial y^2} + \nu \frac{\partial^2 w}{\partial x^2} \right), \tag{3.1 b}$$

$$M_{xy} = D(1-\nu) \frac{\partial^2 w}{\partial x \, \partial y}, \tag{3.1 c}$$

where D is the flexural rigidity and ν is Poisson's ratio. When these equations are substituted into the equations of element equilibrium we obtain, in the absence of normal loading, the following partial differential equation

$$\frac{\partial^4 w}{\partial x^4} + 2 \frac{\partial^4 w}{\partial x^2 \partial y^2} + \frac{\partial^4 w}{\partial y^4} = 0, \tag{3.2}$$
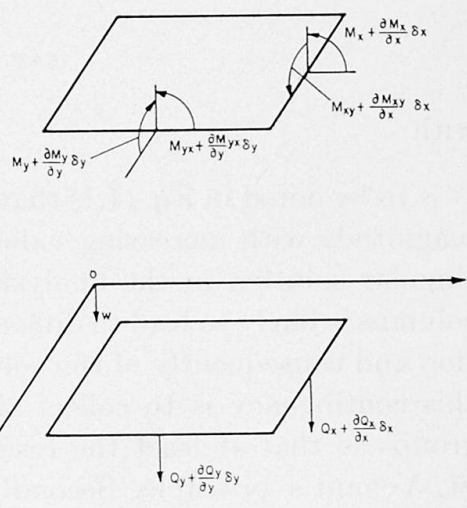
which governs the behaviour of the plate.

Fig. 1. Bending moments and shearing forces acting on an elemental portion of plate.

The normal shearing forces are given by

$$Q_x = -D \frac{\partial}{\partial x} \left(\frac{\partial^2 w}{\partial x^2} + \frac{\partial^2 w}{\partial y^2} \right), \tag{3.3 a}$$

$$Q_y = -D \frac{\partial}{\partial y} \left(\frac{\partial^2 w}{\partial x^2} + \frac{\partial^2 w}{\partial y^2} \right), \tag{3.3 b}$$

and the Kirchhoff normal forces by

$$V_x = Q_x - \frac{\partial M_{xy}}{\partial y} = -D \frac{\partial}{\partial x} \left\{ \frac{\partial^2 w}{\partial x^2} + (2-\nu) \frac{\partial^2 w}{\partial y^2} \right\}, \tag{3.4 a}$$

$$V_y = Q_y - \frac{\partial M_{xy}}{\partial x} = -D \frac{\partial}{\partial y} \left\{ \frac{\partial^2 w}{\partial y^2} + (2-\nu) \frac{\partial^2 w}{\partial x^2} \right\}. \tag{3.4 b}$$

4. Force Groups

The rectangular plate is supported on l distinct columns all of which are here considered to be rigid and to rest upon rigid foundations which may, however, have already settled a prescribed amount. The boundary is free from all traction and restraint.

For the present purpose these columns are replaced by l concentrated reactive forces of such intensity that the deflection $w(x, y)$ of the loaded plate is allowed to take up just the prescribed settlement at the column positions. Now, there are only three equations of overall equilibrium and so the calculation of the intensity of these reactive forces provides a $l-3$ fold statically indeterminate problem which is additional to the usual boundary value problem presented by the rectangular plate.

The singular solution of the governing partial differential Eq. (3.2) appropriate to a concentrated force of unit intensity acting at the origin of co-ordinates in a plate of finite extent is

$$w(x, y) = \frac{1}{16 \pi D} r^2 \log r^2 \tag{4.1}$$

with
$$r^2 = x^2 + y^2. \tag{4.2}$$

It is to be noted in Eq. (4.1) that the deflection $w(x, y)$ increases very rapidly in magnitude with increasing values of r. Clearly, the direct use of this type of singular solution in the analysis of a plate supported by a large number of columns is likely to lead to difficulty in calculating accurate values of the deflection and consequently of the column reactions. A first step in guarding against this contingency is to collect the reactive forces into self-equilibrating force groups so that at least the resulting stress disturbances behave according to St. Venant's principle. Secondly, advantage is often obtained by algebraic rearrangement of the equations in such a way as to reduce likelihood of the occurrence of differences between numerical values of similar magnitude during the course of the computation. Such rearrangement does not of necessity result in an equation possessing the simplest algebraic reduction.

4.1. Force Groups F_α for the Statically Indeterminate Quantities

Linearly independent force groups F_α are introduced as the statically indeterminate quantities for the column reactive forces where

$$F_\alpha = - \sum_{m=1}^{l} c_{\alpha m} p_m, \quad \alpha = 1, 2, 3, \ldots l-3. \tag{4.3}$$

The symbol p_m refers to a concentrated load of unit magnitude acting downwards, i. e. in the sense described in Section 3, at the position $x = x_m$, $y = y_m$ which was previously occupied by column m; the $c_{\alpha m}$ are constants where a

positive value corresponds with a column compression. Other linearly indepen-
dent force groups, such as $\overline{F}_\alpha$, may be obtained through a linear combination of
the F_α so that

$$\overline{F}_\alpha = \sum_{m=1}^{l-3} \overline{c}_{\alpha m} F_m, \tag{4.4}$$

where the $\overline{c}_{\alpha m}$ are constants. This arbitrary choice of the statically indetermi-
nate quantities can be used to considerable advantage.

If each force group F_α is self-equilibrating and is confined to the four
(adjacent) column positions $m = i, j, k, k'$ as shown in Fig. 2 (or $m = i, j, k$ if these

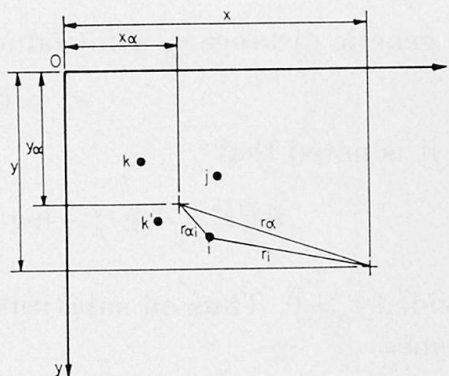Fig. 2. Notation for the force group F_α
at adjacent column positions i, j, k, k'.

positions are co-linear), then

$$F_\alpha = -(c_{\alpha i} p_i + c_{\alpha j} p_j + c_{\alpha k} p_k + c_{\alpha k'} p_{k'}) \tag{4.5}$$

with the remaining $c_{\alpha m} \equiv 0$. For equilibrium it is necessary that

$$\begin{aligned}
c_{\alpha j} + c_{\alpha k} + c_{\alpha k'} &= -c_{\alpha i}, \\
x_j c_{\alpha j} + x_k c_{\alpha k} + x_{k'} c_{\alpha k'} &= -x_i c_{\alpha i}, \\
y_j c_{\alpha j} + y_k c_{\alpha k} + y_{k'} c_{\alpha k'} &= -y_i c_{\alpha i},
\end{aligned} \tag{4.6}$$

where $c_{\alpha i}$ may be taken as unity. This force group gives rise to a stress distur-
bance which, by St. Venant's principle, decreases in magnitude with increasing
distance away from the group. The singular solution of Eq. (3.2) which corre-
sponds with this force group is written $w_\alpha(x, y)$ where

$$w_\alpha(x, y) = \frac{1}{16\pi D} (c_{\alpha i} r_i^2 \log r_i^2 + c_{\alpha j} r_j^2 \log r_j^2 + c_{\alpha k} r_k^2 \log r_k^2 + c_{\alpha k'} r_{k'}^2 \log r_{k'}^2) \tag{4.7}$$

with $\qquad r_i^2 = (x - x_i)^2 + (y - y_i)^2, \qquad r_j^2 = (x - x_j)^2 + (y - y_j)^2 \quad$ etc., $\tag{4.8}$

cf. Eqs. (4.1) and (4.2).

Eq. (4.7) is now rearranged so as to take advantage of the self-equilibrating
properties of the force group, this rearrangement is of especial importance
whenever it is required to calculate the magnitude of w_α at a large distance
away from the group. It is convenient to denote by x_α, y_α some point which lies
within the immediate vicinity of the force group F_α, e. g.

$$x_\alpha = \frac{x_i + x_j + x_k + x_{k'}}{4}, \qquad y_\alpha = \frac{y_i + y_j + y_k + y_{k'}}{4}, \qquad (4.9)$$

see Fig. 2, and to assign to each force group a constant Γ_α which is calculated from the formula

$$\Gamma_\alpha = c_{\alpha i}\, r^2_{\alpha i} + c_{\alpha j}\, r^2_{\alpha j} + c_{\alpha k}\, r^2_{\alpha k} + c_{\alpha k'}\, r^2_{\alpha k'}, \qquad (4.10)$$

where $\quad r^2_{\alpha i} = (x_\alpha - x_i)^2 + (y_\alpha - y_i)^2, \qquad r^2_{\alpha j} = (x_\alpha - x_j)^2 + (y_\alpha - y_j)^2 \quad$ etc. $\quad (4.11)$

In virtue of Eqs (4.6) and (4.8), however, it is noted that we can rewrite Γ_α in the form

$$\Gamma_\alpha = c_{\alpha i}\, r^2_i + c_{\alpha j}\, r^2_j + c_{\alpha k}\, r^2_k + c_{\alpha k'}\, r^2_{k'}. \qquad (4.12)$$

The generic distance r_α is introduced, see Fig. 2, where

$$r^2_\alpha = (x - x_\alpha)^2 + (y - y_\alpha)^2 \qquad (4.13)$$

and it is noted that

$$\log r^2_i = \log r^2_\alpha + \log \frac{r^2_i}{r^2_\alpha}, \qquad \log r^2_j = \log r^2_\alpha + \log \frac{r^2_j}{r^2_\alpha} \quad \text{etc.} \qquad (4.14)$$

provided $r_\alpha \neq 0$. Thus on substituting from Eqs. (4.12) and (4.14) the solution becomes

$$w_\alpha(x, y) = \frac{1}{16\pi D} \left\{ \Gamma_\alpha \log r^2_\alpha + c_{\alpha i}\, r^2_i \log \frac{r^2_i}{r^2_\alpha} + c_{\alpha j}\, r^2_j \log \frac{r^2_j}{r^2_\alpha} \right.$$
$$\left. + c_{\alpha k}\, r^2_k \log \frac{r^2_k}{r^2_\alpha} + c_{\alpha k'}\, r^2_{k'} \log \frac{r^2_{k'}}{r^2_\alpha} \right\}. \qquad (4.15)$$

Furthermore,

$$r^2_j \log \frac{r^2_j}{r^2_\alpha} - r^2_i \log \frac{r^2_i}{r^2_\alpha} = \frac{1}{2} \left\{ (r^2_j + r^2_i) \log \frac{r^2_j}{r^2_i} + (r^2_j - r^2_i) \log \frac{r^2_j\, r^2_i}{r^4_\alpha} \right\}, \qquad (4.16)$$

so that with this equality and the first of Eqs. (4.6), the singular solution $w_\alpha(x, y)$ of Eq. (4.7) is finally rearranged in the form

$$w_\alpha(x, y) = \frac{1}{32\pi D} \left[2\, \Gamma_\alpha \log r^2_\alpha + \left\{ c_{\alpha j}\, (r^2_j + r^2_i) \log \frac{r^2_j}{r^2_i} + c_{\alpha k}\, (r^2_k + r^2_i) \log \frac{r^2_k}{r^2_i} \right. \right.$$
$$\left. + c_{\alpha k'}\, (r^2_{k'} + r^2_i) \log \frac{r^2_{k'}}{r^2_i} \right\} \qquad (4.17)$$
$$+ \left\{ c_{\alpha j}\, (r^2_j - r^2_i) \log \frac{r^2_j\, r^2_i}{r^4_\alpha} + c_{\alpha k}\, (r^2_k - r^2_i) \log \frac{r^2_k\, r^2_i}{r^4_\alpha} + c_{\alpha k'}\, (r^2_{k'} - r^2_i) \log \frac{r^2_{k'}\, r^2_i}{r^4_\alpha} \right\} \right].$$

In this equation, the term in Γ_α is dominant for the large values of r_α and for particularly difficult calculations it may be necessary to derive another set of force groups $\overline{F}_\alpha$, see Eq. (4.4), in the manner

$$\overline{F}_\alpha = \Gamma_{\alpha'} F_\alpha - \Gamma_\alpha F_{\alpha'}, \qquad (4.18)$$

where F_α and $F_{\alpha'}$ are two immediately adjacent self-equilibrating force groups with $r_\alpha = r_{\alpha'}$ and which are individually determined in the normal way from

Eq. (4.6). The terms enclosed in the final pair of braces in Eq. (4.17) are insignificant for very large values of r_α.

4.2. Force Groups F_β for the Applied Loading

In addition to the force groups for the statically indeterminate quantities, principal force groups F_β must be selected to deal with the applied loading and which is here considered to consist of concentrated loads l' in number.

The concentrated applied load $c_{\beta i} p_i$, which acts downwards with intensity $c_{\beta i}$ at the point $x = x_i$, $y = y_i$, is considered for the present purpose to be reacted entirely by the adjacent columns j, k, k'. Thus, a self-equilibrating principal force group F_β is given by

$$F_\beta = c_{\beta i} p_i - c_{\beta j} p_j - c_{\beta k} p_k - c_{\beta k'} p_{k'}, \tag{4.19}$$

where a positive value of $c_{\beta j}$, $c_{\beta k}$, $c_{\beta k'}$ corresponds with column compression and they are calculated from the equilibrium equations

$$
\begin{aligned}
c_{\beta j} + c_{\beta k} + c_{\beta k'} &= c_{\beta i}, \\
x_j c_{\beta j} + x_k c_{\beta k} + x_{k'} c_{\beta k'} &= x_i c_{\beta i}, \\
y_j c_{\beta j} + y_k c_{\beta k} + y_{k'} c_{\beta k'} &= y_i c_{\beta i},
\end{aligned} \tag{4.20}
$$

cf. Eqs. (4.5) and (4.6) for the statically indeterminate quantities.

The singular solution $w_\beta(x, y)$ which corresponds with this principal force group is

$$
\begin{aligned}
w_\beta(x, y) = \frac{1}{32 \pi D} & \left[2 \Gamma_\beta \log r_\beta^2 + \left\{ c_{\beta j} (r_j^2 + r_i^2) \log \frac{r_j^2}{r_i^2} + c_{\beta k} (r_k^2 + r_i^2) \log \frac{r_k^2}{r_i^2} \right. \right. \\
& \left. + c_{\beta k'} (r_{k'}^2 + r_i^2) \log \frac{r_{k'}^2}{r_i^2} \right\} \\
& \left. + \left\{ c_{\beta j} (r_j^2 - r_i^2) \log \frac{r_j^2 r_i^2}{r_\beta^4} + c_{\beta k} (r_k^2 - r_i^2) \log \frac{r_k^2 r_i^2}{r_\beta^4} + c_{\beta k'} (r_{k'}^2 - r_i^2) \log \frac{r_{k'}^2 r_i^2}{r_\beta^4} \right\} \right],
\end{aligned} \tag{4.21}
$$

cf. Eq. (4.17). The constant Γ_β is calculated from the formula

$$\Gamma_\beta = -c_{\beta i} r_{\beta i}^2 + c_{\beta j} r_{\beta j}^2 + c_{\beta k} r_{\beta k}^2 + c_{\beta k'} r_{\beta k'}^2 \tag{4.22}$$

and the quantities x_β and y_β, $r_{\beta i}$, r_β are given respectively by Eqs. (4.9), (4.11) and (4.13) with β substituted for α.

5. Statically Indeterminate Problem of the Infinite Plate

The aforegoing enables the solution to the statically indeterminate problem of the infinite plate which is undergoing the same applied loading and prescribed column settlements as in the actual finite plate. This solution is denoted by $w_{inf}(x, y)$ where

$$w_{inf}(x,y) = \sum_{\beta=1}^{l'} w_\beta(x,y) + \sum_{\alpha=1}^{l-3} C_\alpha w_\alpha(x,y) + C_{l-2}x + C_{l-1}y + C_l, \qquad (5.1)$$

where $w_\alpha(x,y)$ and $w_\beta(x,y)$ are given respectively by Eqs. (4.17) and (4.21) and the C_α are constants. The terms $C_{l-2}x$, $C_{l-1}y$ and C_l account for the rigid body movements of the plate.

If the prescribed settlement for column i is written $w_{col\,set}(x_i,y_i)$ the constants C_α are then determined from the requirement that

$$w_{inf}(x_i,y_i) = w_{col\,set}(x_i,y_i), \qquad i = 1,2,3,\ldots l. \qquad (5.2)$$

This provides the following set of $l \times l$ simultaneous equations

$$\begin{bmatrix} w_1(x_1,y_1) & w_2(x_1,y_1)\ldots w_\alpha(x_1,y_1)\ldots w_{l-3}(x_1,y_1) & x_1 & y_1 & 1 \\ w_1(x_2,y_2) & w_2(x_2,y_2)\ldots w_\alpha(x_2,y_2)\ldots w_{l-3}(x_2,y_2) & x_2 & y_2 & 1 \\ \cdots\cdots\cdots\cdots\cdots\cdots\cdots\cdots\cdots\cdots\cdots\cdots\cdots\cdots\cdots\cdots \\ w_1(x_l,y_l) & w_2(x_l,y_l)\ldots w_\alpha(x_l,y_l)\ldots w_{l-3}(x_l,y_l) & x_l & y_l & 1 \end{bmatrix} \begin{bmatrix} C_1 \\ C_2 \\ \cdot\cdot \\ C_l \end{bmatrix} =$$

$$\begin{bmatrix} w_{col\,set}(x_1,y_1) - \sum_{\beta=1}^{l'} w_\beta(x_1,y_1) \\ w_{col\,set}(x_2,y_2) - \sum_{\beta=1}^{l'} w_\beta(x_2,y_2) \\ \cdots\cdots\cdots\cdots\cdots\cdots \\ w_{col\,set}(x_l,y_l) - \sum_{\beta=1}^{l'} w_\beta(x_l,y_l) \end{bmatrix}. \qquad (5.3)$$

If the statically indeterminate force groups F_α are chosen in the manner described in Section 4 then the square matrix on the L.H.S. of Eq. (5.3) should be well conditioned, but if there is any doubt it is worthwhile repeating the calculation using a different arrangement of force groups, see Eq. (4.4), and to check whether there is any significant change in the final values for the column reactions. The force group which provides for this infinite plate solution is written F_{inf}. It is calculated from

$$F_{inf} = \sum_{\beta=1}^{l'} F_\beta + \sum_{\alpha=1}^{l-3} C_\alpha F_\alpha, \qquad (5.4)$$

where F_α and F_β are as given by Eqs. (4.5) and (4.19) and the values of the constants C_α have just been determined. The force group F_{inf} is, of course, a vector quantity with l components and, according to the convention adopted throughout the present paper, a positive value of a component corresponds with a column compression.

The inversion of the square matrix on the L.H.S. of Eq. (5.3) is used frequently during the iterative process, later described, to provide by matrix multiplication another infinite plate solution which is denoted by $w_{inf}^{(F)}(x,y)$. Thus

$$w_{inf}^{(F)}(x,y) = \sum_{\alpha=1}^{l-3} C_\alpha^{(F)} w_\alpha(x,y) + C_{l-2}^{(F)} x + C_{l-1}^{(F)} y + C_l^{(F)}, \tag{5.5}$$

where the constants $C_\alpha^{(F)}$ are formally calculated from the following set of $l \times l$ simultaneous equations

$$\begin{bmatrix} w_1(x_1,y_1) & w_2(x_1,y_1) \ldots w_\alpha(x_1,y_1) \ldots w_{l-3}(x_1,y_1) & x_1 & y_1 & 1 \\ w_1(x_2,y_2) & w_2(x_2,y_2) \ldots w_\alpha(x_2,y_2) \ldots w_{l-3}(x_2,y_2) & x_2 & y_2 & 1 \\ \cdots \cdots \cdots \cdots \cdots \cdots \cdots \cdots \cdots \cdots \cdots \cdots \cdots \\ w_1(x_l,y_l) & w_2(x_l,y_l) \ldots w_\alpha(x_l,y_l) \ldots w_{l-3}(x_l,y_l) & x_l & y_l & 1 \end{bmatrix} \begin{bmatrix} C_1^{(F)} \\ C_2^{(F)} \\ \cdots \\ C_l^{(F)} \end{bmatrix} =$$

$$\begin{bmatrix} w_{inf}^{(F)}(x_1,y_1) \\ w_{inf}^{(F)}(x_2,y_2) \\ \cdots \cdots \cdots \\ w_{inf}^{(F)}(x_l,y_l) \end{bmatrix}. \tag{5.6}$$

6. Residual Forces Acting at the Boundary of the Rectangular Plate

In preparation for dealing with the boundary value problem of the rectangular plate, it is necessary to calculate the values of the forces which arise from the infinite plate solutions of Section 5 and which act along the lines marking out the rectangular boundary, as shown in Fig. 3.
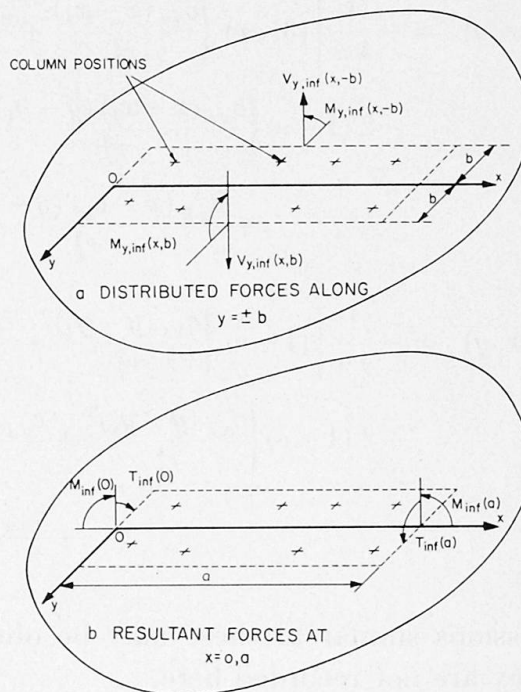

Fig. 3a and b. Residual forces acting at the boundary of the rectangular plate.

We first derive the expressions appropriate to the force group F_α. They are obtained by substituting Eq. (4.7) into Eqs. (3.1) and (3.4) and making use of the equilibrium Eq. (4.6) so that

$$M_{x,\alpha}(x,y) = -\frac{1}{8\pi}\left[(1+\nu)\left\{c_{\alpha j}\log\frac{r_j^2}{r_i^2}+c_{\alpha k}\log\frac{r_k^2}{r_i^2}+c_{\alpha k'}\log\frac{r_{k'}^2}{r_i^2}\right\}\right.$$

$$-2(1-\nu)\left\{\frac{c_{\alpha i}(y-y_i)^2}{r_i^2}+\frac{c_{\alpha j}(y-y_j)^2}{r_j^2}\right. \tag{6.1a}$$

$$\left.\left.+\frac{c_{\alpha k}(y-y_k)^2}{r_k^2}+\frac{c_{\alpha k'}(y-y_{k'})^2}{r_{k'}^2}\right\}\right],$$

$$M_{y,\alpha}(x,y) = -\frac{1}{8\pi}\left[(1+\nu)\left\{c_{\alpha j}\log\frac{r_j^2}{r_i^2}+c_{\alpha k}\log\frac{r_k^2}{r_i^2}+c_{\alpha k'}\log\frac{r_{k'}^2}{r_i^2}\right\}\right.$$

$$+2(1-\nu)\left\{\frac{c_{\alpha i}(y-y_i)^2}{r_i^2}+\frac{c_{\alpha j}(y-y_j)^2}{r_j^2}\right. \tag{6.1b}$$

$$\left.\left.+\frac{c_{\alpha k}(y-y_k)^2}{r_k^2}+\frac{c_{\alpha k'}(y-y_{k'})^2}{r_{k'}^2}\right\}\right],$$

$$M_{xy,\alpha}(x,y) = \frac{1-\nu}{4\pi}\left\{\frac{c_{\alpha i}(x-x_i)(y-y_i)}{r_i^2}+\frac{c_{\alpha j}(x-x_j)(y-y_j)}{r_j^2}\right.$$

$$\left.+\frac{c_{\alpha k}(x-x_k)(y-y_k)}{r_k^2}+\frac{c_{\alpha k'}(x-x_{k'})(y-y_{k'})}{r_{k'}^2}\right\} \tag{6.1c}$$

and

$$V_{x,\alpha}(x,y) = -\frac{1}{4\pi}\left[(3-\nu)\left\{\frac{c_{\alpha i}(x-x_i)}{r_i^2}+\frac{c_{\alpha j}(x-x_j)}{r_j^2}+\frac{c_{\alpha k}(x-x_k)}{r_k^2}+\frac{c_{\alpha k'}(x-x_{k'})}{r_{k'}^2}\right\}\right.$$

$$-2(1-\nu)\left\{\frac{c_{\alpha i}(x-x_i)(y-y_i)^2}{r_i^2}+\frac{c_{\alpha j}(x-x_j)(y-y_j)^2}{r_j^2}\right. \tag{6.2a}$$

$$\left.\left.+\frac{c_{\alpha k}(x-x_k)(y-y_k)^2}{r_k^2}+\frac{c_{\alpha k'}(x-x_{k'})(y-y_{k'})^2}{r_{k'}^2}\right\}\right],$$

$$V_{y,\alpha}(x,y) = -\frac{1}{4\pi}\left[(1-\nu)\left\{\frac{c_{\alpha i}(y-y_i)}{r_i^2}+\frac{c_{\alpha j}(y-y_j)}{r_j^2}+\frac{c_{\alpha k}(y-y_k)}{r_k^2}+\frac{c_{\alpha k'}(y-y_{k'})}{r_{k'}^2}\right\}\right.$$

$$+2(1-\nu)\left\{\frac{c_{\alpha i}(y-y_i)^3}{r_i^4}+\frac{c_{\alpha j}(y-y_j)^3}{r_j^4}\right. \tag{6.2b}$$

$$\left.\left.+\frac{c_{\alpha k}(y-y_k)^3}{r_k^4}+\frac{c_{\alpha k'}(y-y_{k'})^3}{r_{k'}^4}\right\}\right].$$

Expressions similar to these may be obtained for the principal force groups F_β, they are not recorded here.

The infinite plate solution of Eq. (5.1) therefore produces the bending moment

$$M_{y,inf}(x,y) = \sum_{\beta=1}^{l'} M_{y,\beta}(x,y) + \sum_{\alpha=1}^{l-3} C_\alpha M_{y,\alpha}(x,y) \tag{6.3a}$$

and the Kirchhoff normal force

$$V_{y,\,inf}(x,y) = \sum_{\beta=1}^{l'} V_{y,\beta}(x,y) + \sum_{\alpha=1}^{l-3} C_\alpha V_{y,\alpha}(x,y) \tag{6.3 b}$$

along lines of constant y, see Fig. 3a. Similarly, the infinite plate solution of Eq. (5.5) produces

$$M_{y,\,inf}^{(F)}(x,y) = \sum_{\alpha=1}^{l-3} C_\alpha^{(F)} M_{y,\alpha}(x,y) \tag{6.4 a}$$

and

$$V_{y,\,inf}^{(F)}(x,y) = \sum_{\alpha=1}^{l-3} C_\alpha^{(F)} V_{y,\alpha}(x,y) \tag{6.4 b}$$

along lines of constant y.

The ends of the rectangular plate are located along the lines $x=0$, $x=a$. It is now assumed that the plate is very long, i. e. $a/(2\,b) \gg 1$, and that there are no columns or applied loads in the vicinity of the ends. Thus, the residual forces which arise along $x=0$, $x=a$ from the infinite plate solutions of Eqs. (5.1) and (5.5) are small in comparison with those which arise along $y = \pm b$. Moreover, the column reactions are virtually independent of the manner in which these small residual forces are distributed. Accordingly, in what follows we concern ourselves with the calculation of the resultant forces at the ends, i. e. $M_{inf}(0)$, $T_{inf}(0)$ at $x=0$ and $M_{inf}(a)$, $T_{inf}(a)$ at $x=a$ as shown in Fig. 3b.

To determine the resultant bending moment $M_{inf}(x)$ it is first necessary to integrate $M_{x,\alpha}(x,y)$, Eq. (6.1a) over the width $2\,b$ of the plate, so that

$$M_\alpha(x) = \int_{-b}^{b} M_{x,\alpha}(x,y)\,dy, \tag{6.5 a}$$

$$
\begin{aligned}
= -\frac{1}{16\,\pi}\Bigg[& (1+\nu)\Big\{ c_{\alpha j}(2\,y-y_j-y_i)\log\frac{r_j^2}{r_i^2} + c_{\alpha k}(2\,y-y_k-y_i)\log\frac{r_k^2}{r_i^2} \\
& + c_{\alpha k'}(2\,y-y_{k'}-y_i)\log\frac{r_{k'}^2}{r_i^2}\Big\} \\
& -(1+\nu)\{ c_{\alpha j}(y_j-y_i)\log r_j^2 r_i^2 + c_{\alpha k}(y_k-y_i)\log r_k^2 r_i^2 \\
& + c_{\alpha k'}(y_{k'}-y_i)\log r_{k'}^2 r_i^2\} \\
& +8\Big\{ c_{\alpha i}(x-x_i)\tan^{-1}\!\Big(\frac{y-y_i}{x-x_i}\Big) + c_{\alpha j}(x-x_j)\tan^{-1}\!\Big(\frac{y-y_j}{x-x_j}\Big) \\
& + c_{\alpha k}(x-x_k)\tan^{-1}\!\Big(\frac{y-y_k}{x-x_k}\Big) + c_{\alpha k'}(x-x_{k'})\tan^{-1}\!\Big(\frac{y-y_{k'}}{x-x_{k'}}\Big)\Big\}\Bigg]_{y=-b}^{y=b}.
\end{aligned}
\tag{6.5 b}
$$

For the resultant torsion $T_{inf}(x)$ it is necessary to combine the contributions from the corner reactions $2\,M_{xy,\alpha}(x,y)$, Eq. (6.1c), and the Kirchhoff normal force $V_{x,\alpha}(x,y)$ of Eq. (6.2a). Thus

$$T_\alpha(x) = [\int y\, V_{x,\alpha}(x,y)\, dy + 2\, y\, M_{xy,\alpha}(x,y)]_{y=-b}^{y=b}, \tag{6.6a}$$

$$\begin{aligned}
&= -\frac{1}{16\,\pi}\Bigg[(1+\nu)\Bigg\{c_{\alpha j}\,(2\,x-x_j-x_i)\log\frac{r_j^2}{r_i^2}+c_{\alpha k}\,(2\,x-x_k-x_i)\log\frac{r_k^2}{r_i^2}\\
&\qquad\qquad +c_{\alpha k'}\,(2\,x-x_{k'}-x_i)\log\frac{r_{k'}^2}{r_i^2}\Bigg\}\\
&\quad -(1+\nu)\{c_{\alpha j}\,(x_j-x_i)\log r_j^2\,r_i^2+c_{\alpha k}\,(x_k-x_i)\log r_k^2\,r_i^2\\
&\qquad\qquad +c_{\alpha k'}\,(x_{k'}-x_i)\log r_{k'}^2\,r_i^2\}\\
&\quad +8\Bigg\{c_{\alpha i}\,y_i\tan^{-1}\!\left(\frac{y-y_i}{x-x_i}\right)+c_{\alpha j}\,y_j\tan^{-1}\!\left(\frac{y-y_j}{x-x_j}\right)\\
&\qquad\qquad +c_{\alpha k}\,y_k\tan^{-1}\!\left(\frac{y-y_k}{x-x_k}\right)+c_{\alpha k'}\,y_{k'}\tan^{-1}\!\left(\frac{y-y_{k'}}{x-x_{k'}}\right)\Bigg\}\\
&\quad -4\,y\,(1-\nu)\Bigg\{\frac{c_{\alpha i}\,(x-x_i)\,(y-y_i)}{r_i^2}+\frac{c_{\alpha j}\,(x-x_j)\,(y-y_j)}{r_j^2}\\
&\qquad\qquad +\frac{c_{\alpha k}\,(x-x_k)\,(y-y_k)}{r_k^2}+\frac{c_{\alpha k'}\,(x-x_{k'})\,(y-y_{k'})}{r_{k'}^2}\Bigg\}\Bigg]_{y=-b}^{y=b}.
\end{aligned} \tag{6.6b}$$

Expressions similar to these may be obtained for the principal force groups F_β, they are not recorded here.

The infinite plate solution of Eq. (5.1) therefore produces the resultant bending moment

$$M_{inf}(x) = \sum_{\beta=1}^{l'} M_\beta(x) + \sum_{\alpha=1}^{l-3} C_\alpha M_\alpha(x) \tag{6.7a}$$

and the resultant torsion

$$T_{inf}(x) = \sum_{\beta=1}^{l'} T_\beta(x) + \sum_{\alpha=1}^{l-3} C_\alpha T_\alpha(x). \tag{6.7b}$$

Similarly, the infinite plate solution of Eq. (5.5) produces the resultant bending moment

$$M_{inf}^{(F)}(x) = \sum_{\alpha=1}^{l-3} C_\alpha^{(F)} M_\alpha(x) \tag{6.8a}$$

and the resultant torsion

$$T_{inf}^{(F)}(x) = \sum_{\alpha=1}^{l-3} C_\alpha^{(F)} T_\alpha(x). \tag{6.8b}$$

7. Fourier Analysis of the Unrestrained Rectangular Plate

We deal now with the boundary value problem of the rectangular plate which is loaded by a system of self-equilibrating forces acting at the boundary, as shown in Fig. 3. The columns are removed for this purpose so that the plate is completely unrestrained and this provides a straight-forward problem which can be solved in a number of ways.

The Fourier method of solution is chosen because of the advantages of the orthogonal relationship and the simplifications which arise if the plate is of sufficient length so that the behaviour at the column positions is independent of the way in which the forces are distributed at the ends $x = 0, a$. This simplified Fourier solution is written $w^{(F)}(x, y)$ with

$$w^{(F)}(x, y) =$$

$$- \frac{1}{12\, b\, D\, (1 - \nu^2)} \left[3\, (x^2 - \nu\, y^2)\, M_{inf}(0) + (x^3 - 3\, \nu\, x\, y^2) \frac{M_{inf}(a) - M_{inf}(0)}{a} \right]$$

$$+ \frac{1}{8\, b\, D\, (1 - \nu)} \left[2\, x\, y\, T_{inf}(0) + x^2\, y\, \frac{T_{inf}(a) - T_{inf}(0)}{a} \right] \tag{7.1}$$

$$+ \frac{1}{16\, \pi\, D} \left[A_0 + B_0\, x + \sum_{n=1}^{\infty} \left(A_n \cosh \gamma_n y + \frac{B_n y}{b} \sinh \gamma_n y \right) \frac{\sin \gamma_n x}{\cosh \gamma_n b} \right]$$

$$+ \frac{1}{16\, \pi\, D} \left[C_0\, y + D_0\, y^3 + \sum_{n=1}^{\infty} \left(C_n \sinh \gamma_n y + \frac{D_n y}{b} \cosh \gamma_n y \right) \frac{\cos \gamma_n x}{\cosh \gamma_n b} \right],$$

where
$$\gamma_n = n\, \pi / a. \tag{7.2}$$

In Eq. (7.1) it is noted that the first series is symmetrical in y and contributes nothing to the deflection $w^{(F)}(x, y)$ at the ends, while the second series is antisymmetrical in y and does not contribute to the warping at the ends $x = 0, a$. The A_n, B_n, C_n, D_n are constants to be determined so that the boundary conditions are satisfied; in particular A_0, B_0, C_0 control the rigid body movements and may be adjusted to minimize the absolute magnitude of the deflections at the column positions. If Eq. (7.1) is substituted into the equations of Section 3 and use made of equations like (6.5 a) and (6.6 b) it can be checked that the conditions for the resultant forces are satisfied at the ends $x = 0, a$.

The (residual) bending moments $M_{y, inf}$ and (residual) Kirchhoff normal forces $V_{y, inf}$ which act along the boundaries $y = \pm b$ are easily expanded into a Fourier sine, or cosine, series by the method described by HILDEBRAND [9]. Thus the A_n and B_n are obtained from

$$\begin{bmatrix} \gamma_n^2 (1 - \nu) & \gamma_n \left\{ \dfrac{2}{b} + \gamma_n (1 - \nu) \tanh \gamma_n b \right\} \\[2ex] -\gamma_n^3 (1 - \nu) \tanh \gamma_n b & \gamma_n^2 \left\{ \dfrac{1}{b} (1 + \nu) \tanh \gamma_n b - \gamma_n (1 - \nu) \right\} \end{bmatrix} \begin{bmatrix} A_n \\[2ex] B_n \end{bmatrix} =$$

$$\begin{bmatrix} -\dfrac{16\,\pi}{a} \displaystyle\int_0^a \{ M_{y, inf}(x, b) + M_{y, inf}(x, -b) \} \sin \gamma_n x\, dx \\[3ex] -\dfrac{16\,\pi}{a} \displaystyle\int_0^a \{ V_{y, inf}(x, b) - V_{y, inf}(x, -b) \} \sin \gamma_n x\, dx \end{bmatrix} \tag{7.3}$$

and the C_n and D_n from

$$
\begin{bmatrix}
\gamma_n^2 (1-\nu) \tanh \gamma_n b & \gamma_n \left\{ \dfrac{2}{b} \tanh \gamma_n b + \gamma_n (1-\nu) \right\} \\[2ex]
-\gamma_n^3 (1-\nu) & \gamma_n^2 \left\{ \dfrac{1}{b} (1+\nu) - \gamma_n (1-\nu) \tanh \gamma_n b \right\}
\end{bmatrix}
\begin{bmatrix} C_n \\[2ex] D_n \end{bmatrix}
=
$$

$$
\begin{bmatrix}
-\dfrac{16\,\pi}{a} \displaystyle\int_0^a \{ M_{y,inf}(x,b) - M_{y,inf}(x,-b) \} \cos \gamma_n x \, dx \\[3ex]
-\dfrac{16\,\pi}{a} \displaystyle\int_0^a \{ V_{y,inf}(x,b) + V_{y,inf}(x,-b) \} \cos \gamma_n x \, dx
\end{bmatrix} . \tag{7.4}
$$

Finally, for the constant D_0 we have

$$
\begin{bmatrix}
\dfrac{2\,\pi\,\nu}{a\,b\,(1-\nu)} & 3 \\[2ex]
\dfrac{2\,\pi\,(2-\nu)}{a\,b\,(1-\nu)} & 3
\end{bmatrix}
\begin{bmatrix}
T_{inf}(a) - T_{inf}(0) \\[2ex]
D_0
\end{bmatrix}
=
\begin{bmatrix}
-\dfrac{4\,\pi}{a\,b} \displaystyle\int_0^a \{ M_{y,inf}(x,b) - M_{y,inf}(x,-b) \} \, dx \\[3ex]
-\dfrac{4\,\pi}{a} \displaystyle\int_0^a \{ V_{y,inf}(x,b) + V_{y,inf}(x,-b) \} \, dx
\end{bmatrix} ,
$$

$$\tag{7.5}$$

which provides also an alternative derivation of the quantity $T_{inf}(a) - T_{inf}(0)$, see Eqs. (6.7b) and (6.8b).

8. The Iterative Process

The broad outline of the iterative process is described in the Introduction. The statically indeterminate solution $w_{inf}(x,y)$ of Eq. (5.1) is obtained for the infinite plate under the prescribed loading and prescribed column settlements. In preparation for the first iterate, we calculate the residual bending moment $M_{\nu,inf}(x,y)$ of Eq. (6.3a) together with the Kirchhoff normal force $V_{\nu,inf}(x,y)$ of Eq. (6.3b) along the lines which mark out the boundary of the rectangular plate, see Fig. 3, where the symbol ν denotes here the outward normal to the boundary. We set

$$
M_{\nu,inf}^{(F)}(x,y) = M_{\nu,inf}(x,y) \tag{8.1a}
$$

and
$$
V_{\nu,inf}^{(F)}(x,y) = V_{\nu,inf}(x,y) \tag{8.1b}
$$

and so obtain the Fourier solution $w^{(F)}(x,y)$ of Eq. (7.1). This Fourier solution is, in its turn, used to derive a new infinite plate solution $w_{inf}^{(F)}(x,y)$, see Eq. (5.5), by setting

$$
w_{inf}^{(F)}(x_i,y_i) = w^{(F)}(x_i,y_i) \tag{8.2}
$$

at each column position $i = 1, 2 \ldots l$. The aforegoing equations are now com-

bined to provide a first approximation $w'(x, y)$ to the solution of the boundary value problem of the column supported rectangular plate where

$$w'(x, y) = w_{inf}(x, y) - \lambda' w^{(F)}(x, y) + \lambda' w_{inf}^{(F)}(x, y). \tag{8.3}$$

The value of the constant λ' remains to be chosen, but it must fall within the range $0 < \lambda' \leqq 1$. Eq. (8.3), provides bending moments M'_ν around the rectangular boundary

$$M'_\nu = M_{\nu, inf} - \lambda' M_\nu^{(F)} + \lambda' M_{\nu, inf}^{(F)} \tag{8.4}$$

and similarly for the Kirchhoff normal forces and concentrated corner reactions and, in preparation for assigning a value to λ', it is useful to calculate the quantity

$$\Lambda' = \frac{\int\limits_C M_{\nu, inf} (M_\nu^{(F)} - M_{\nu, inf}^{(F)})\, ds}{\int\limits_C (M_\nu^{(F)} - M_{\nu, inf}^{(F)})^2\, ds}, \tag{8.5}$$

because this provides a valuable indication of the convergence of the iterative process. In Eq. (8.5), C denotes the boundary of the rectangular plate and s the distance measured around this boundary.

Let us now consider the philosophy which underlies the iteration procedure. If all the columns and applied loads are at a great distance from the boundary then the residual boundary tractions are so small that an accurate solution is obtained after only one iterate, see Eqs. (8.1) to (8.3), simply by setting $\lambda' = 1$. In practice, however, the boundary at $y = \pm b$ is usually in the vicinity of some of the applied loads and/or columns and it must be recognized that, in this case, the true corrective tractions at the boundary bear only a qualitative relationship with the residual tractions which we have calculated from the solution for the infinite plate. Indeed, if λ' is now taken as unity then the solution $w'(x, y)$ of Eq. (8.3) may well be a worse approximation than that given by $w_{inf}(x, y)$ alone. One remedy is, of course to extend the whole boundary and then to solve the boundary value problems which are presented in succession by incremental contraction of the boundary back to its original contour. This is, however, inconvenient from the computational point of view, it is much easier to simulate crudely this effect by taking values of λ' smaller than unity. If we put $\lambda' = \Lambda'$, see Eq. (8.5) then this minimizes the error bending moment distribution around the boundary of the rectangular plate but, in practice, it is usually found to be better to put

$$\lambda' = c\Lambda', \tag{8.6}$$

where c is a constant which is prescribed for each problem in the light of experience (typically $0.1 \leqq c \leqq 1.0$). Moreover, it is found that the convergence of the iterative process is accelerated by a simple device as follows. If $w^*(x, y)$ denotes the solution obtained from the previous iterate then it is to be expected that the solution $w(x, y)$, with

$$w(x,y) = \frac{1}{1+\lambda'}\{w^*(x,y)+\lambda' w'(x,y)\}, \tag{8.7}$$

is nearer to the exact solution than either $w^*(x,y)$ or $w'(x,y)$. In the case of the first iterate we put $w^*(x,y)=w_{inf}(x,y)$.

The above process is repeated for the second and successive iterates except only that in Eqs. (8.1) we set

$$M^{(F)}_{\nu,inf}(x,y) = M'_{\nu,inf}(x,y) \tag{8.8a}$$

and
$$V^{(F)}_{\nu,inf}(x,y) = V'_{\nu,inf}(x,y), \tag{8.8b}$$

where the new residual tractions, denoted by the prime, are calculated on the basis that the column settlement $w_{col\,set}(x_i,y_i)$ of Eq. (5.2) is modified by the amount

$$\frac{1}{1+\lambda'}\{w_F(x_i,y_i)+\lambda' w'_F(x_i,y_i)\}$$

with $i=1,2\ldots l$. The process is repeated until the quantity Λ' of Eq. (8.5) is sufficiently close to unity, typically $0.9999 \leq \Lambda' \leq 1.0001$ provides a solution of high engineering accuracy. It is sound practice, however, for the ultimate iterate to modify $w_{col\,set}(x_i,y_i)$ by the amount

$$w'_F(x_i,y_i)$$

and to bypass Eq. (8.7) by setting

$$w(x,y) = w'(x,y) \tag{8.9}$$

and then to compare the values of the column reactions so obtained with those from the penultimate iterate. This is equivalent to a full, i. e. unfactored, application of the corrective tractions to the boundary of the plate.

9. Numerical Examples and Comparisons with other Results

The question of interpretation and accuracy of results is important. An actual bridge structure is complex and it is always necessary to introduce some simplification, such as by smoothing the geometry or excluding certain effects of three dimensional stress distribution, in order to provide another physical representation which can be solved by one of the established methods of analysis. It is therefore inevitable that inaccuracy occurs when interpreting the numerical results back into terms of the actual structure, the extent of the inaccuracy depending upon the closeness of the physical representation. The engineer has, however, a firm basis upon which to exercise his judgement provided that this inaccuracy is not compounded with unknown error arising from simplifications in the mathematical analysis or from inadequate computation. It is necessary, therefore, to demonstrate the validity both of the preceding analysis and the

computer program and to make comparisons with known results although these are generally available only for a relatively simple class of problem and are generally known to be subject to experimental error or are the results of a finite difference calculation. Indeed, it has not been possible to obtain an absolute comparison by these means because the few results obtained from rigorous mathematical investigation refer either to problems of the classical type (i. e. infinite strip, rectangular plate) where the plate is supported upon continuously distributed bearings and/or the relevant computations are not seen to have been pursued to the extent that a four, or even three, significant accuracy is assured for those physical quantities which are of final interest. Thus, in many of the following comparisons it is necessary to approximate a continuously distributed bearing by a number of discretely spaced columns. Finally, a comparison is made with the results obtained from the model tests which were carried out in connection with the design of the complex bridge structure which forms part of the elevated road system at the Cumberland Basin in Bristol.

As mentioned in the Introduction, no attempt is made in these numerical examples to achieve economy of computer usage and no account is taken of any symmetrical properties which may be present. Instead, a large number of terms is taken in the Fourier series, together with sufficient iterations, in order to be assured of a high standard of accuracy, usually to within four significant figures. Typically, the Fourier series of Eq. (7.1) is truncated between $40 \leqq n \leqq 130$ and, in order to obtain some appreciation of the scale of the calculation, we see that there is some relationship here between the value of n and the fineness of a finite difference or finite element mesh. Thus, if in the latter method the length of the rectangular plate is divided into 100 elemental portions, comparable with $n = 100$, and the width is coarsely divided into only 10 elemental portions then this requires the inversion of an immense matrix, albeit sparse, of order something like 3000×3000. In contrast, the maximum size of matrix which is required to be inverted by the present method is of order $l \times l$ where l is the number of column supports.

The present method in conjunction with the computer program provides a very flexible design tool. Thus, economies of computer usage for design calculations can be achieved by generally using rather smaller values of n and making occasional checks on the accuracy by increasing this value such as for the more critical design cases. Indeed, it is found in the example on the Cumberland Basin elevated roadway that the preliminary infinite plate solution (i. e. $n = 0$), which is itself a fairly trivial calculation, provides a good indication of the actual column reactions. Moreover, since this preliminary infinite plate solution is an explicit and exact calculation, i. e. within the confines of the classical theory of plate bending, the designer is here provided with an immediate and direct physical basis for interpretation. Economies of computer usage can occasionally be obtained by confining attention to the separate local areas of interest — especially in bridges which are of considerable extent.

9.1. *The Cantilever Plate*

This first problem has practical significance in the design of certain types of monorail cranes and was solved by JARAMILLO [10] in 1950 using the Fourier integral method for an infinitely long cantilever plate with a continuous clamped edge. Its approximate representation by a rectangular plate supported upon 13 columns is shown in Fig. 4.
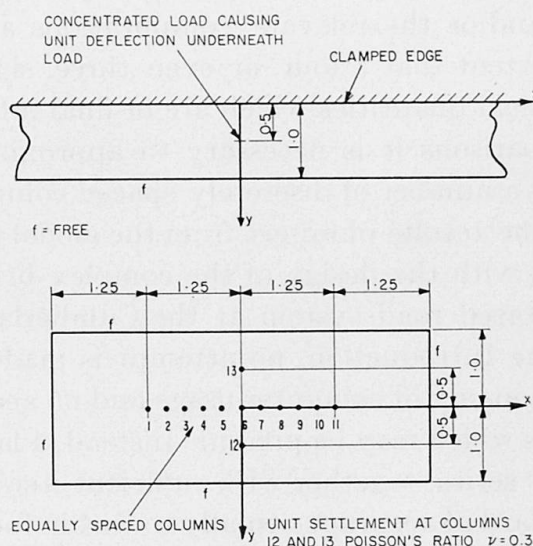

Fig. 4. Representation of a cantilever plate of infinite length under concentrated load.

From JARAMILLO's results it is found that a concentrated load of intensity $158.2\,D$ causes a unit deflection underneath the load whereas the load in columns 12 and 13, for unit settlement of these columns, is obtained from the present computer program as $-154.7\,D$ when the Fourier series of Eq. (7.1) is truncated at $n=40$, it is recalled that D is the flexural rigidity and that a positive load indicates column compression. The difference of just over two per cent between these two values is attributable to the additional restraint which is imposed by the infinitely long plate and the continuous clamped edge.

9.2. *The Square Plate*

The classical problem of the square plate with two opposite edges simply supported and the remaining edges free is important and has been studied by ROBINSON [11], BALAS and HANUSKA [12] and by KURATA and OKAMURA [13] both theoretically and experimentally. ROBINSON uses a straightforward finite difference technique for various mesh sizes, the finest of which divides the plate into 64 elemental squares, whereas BALAS and HANUSKA first remove the singularity introduced by the concentrated load before proceeding with their finite difference analysis with the plate divided into 48 elemental rectangles. KURATA and OKAMURA employ continuous functions in the form of Fourier series.

The classical problem can be approximated by a column supported rectangular plate as shown in Fig. 5 where the continuously supported edges are both replaced by five equally spaced columns. A central concentrated load at $x = 0$, $y = 0$, of unit intensity is simulated, in this instance, by an additional central column which is allowed to settle just enough to produce a unit tension load in that column. This enables a comparison of results for the deflection to be obtained with those from the classical problem and, for this purpose, the Fourier series of Eq. (7.1) is truncated after $n = 60$ and the iterative process continued until there is no change in the fourth significant figure for the reaction in each column.
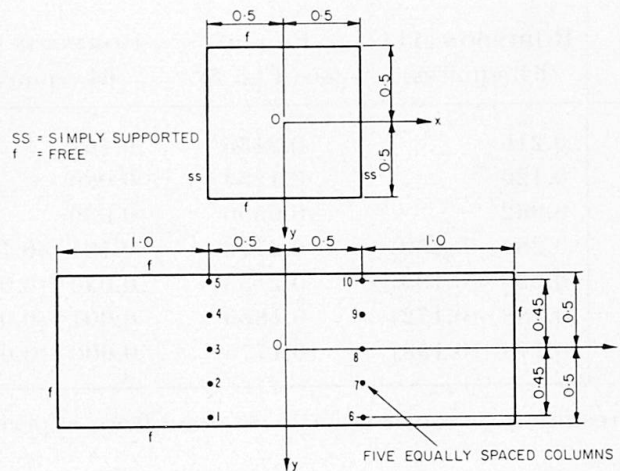
Fig. 5. Representation of a square plate with two opposite edges simply supported and remaining edges free.

Table 1. Deflection w under unit central load in a square plate with two opposite edges simply supported, remaining edges free

Source	Poisson's ratio v	w (theory)	w (experiment)
ROBINSON [11] (64 squares)	0.3	$0.0241/D$	$0.0247/D$
KURATA and OKAMURA [13]	0.3	$0.02320/D$	$0.02253/D$
Present (see Fig. 5)	0.3	$0.02310/D$	—
BALAS and HANUSKA [12]	0.1667	$0.02456/D$	—
Present (see Fig. 5)	0.1667	$0.02316/D$	—

Table 1 provides comparative values of the deflection w underneath the unit central load and it is to be noted that ROBINSON, KURATA and OKAMURA, take Poisson's ratio as $v = 0.3$ whereas BALAS and HANUSKA use $v = 0.1667$. There is agreement to within 0.5 per cent of the theoretical value of KURATA and OKAMURA whereas the theoretical values derived by ROBINSON and BALAS and HANUSKA show a rather greater difference amounting to some 6 per cent. With regard to experiment, the present method provides the closest agreement

118   L. S. D. MORLEY

to the results obtained by KURATA and OKAMURA from their tests on an alumi-
nium plate. Tables 2 and 3 list comparative values of the bending moments
M_x and M_y with those derived from the finite difference calculations of ROBIN-
SON and BALAS and HANUSKA. The differences between the listed maximum
values in the two Tables are respectively 3.5 per cent and 5.3 per cent.

Table 2. *Bending moments M_x and M_y in a square plate with unit central load and two
opposite edges simply supported, remaining edges free. Comparison with Robinson's results.
Poisson's ratio $\nu = 0.3$*

Co-ordinate position (see Fig. 5)		M_x		M_y	
x	y	ROBINSON [11] (64 squares)	Present (see Fig. 5)	ROBINSON [11] (64 squares)	Present (see Fig. 5)
0.125	0	0.216	0.2135	0.161	0.1491
0.250	0	0.126	0.1253	0.086	0.0759
0.375	0	0.062	0.0556	0.039	0.0285
0	0.125	0.287 (0.259)	0.2772	0.101 (0.108)	0.0971
0	0.250	0.220 (0.195)	0.2133	0.036 (0.039)	0.0350
0	0.375	0.188 (0.172)	0.1855	0.007 (0.015)	0.0083
0	0.500	0.178 (0.158)	0.1775	0.000 (0.000)	0.0000

The results in parentheses are obtained from experiment

Table 3. *Bending moments M_x and M_y in a square plate with unit central load and two
opposite edges simply supported, remaining edges free. Comparison with Balas and Hanuska's
results. Poisson's ratio $\nu = 0.1667$*

Co-ordinate position (see Fig. 5)		M_x		M_y	
x	y	BALAS and HANUSKA [12]	Present (see Fig. 5)	BALAS and HANUSKA [12]	Present (see Fig. 5)
0.125	0	0.208	0.2027	0.140	0.1287
0.250	0	0.123	0.1204	0.077	0.0638
0.375	0	0.059	0.0527	0.035	0.0226
0	0.167	0.265	0.2513	0.042	0.0432
0	0.333	0.204	0.1978	0.000	0.0007
0	0.500	0.184	0.1796	0.000	0.0000

Influence surfaces for the column reactions of supported plates, like the rectan-
gular plate shown in Fig. 5 but with the ends located at $-0.5417 \leqq x \leqq 0.5417$, are
provided by MEHMEL and WEISE [14] from numerous experiments on plate glass
models with Poisson's ratio $\nu = 0.228$. For a concentrated load of unit intensity
located at a point $x = 0.375$, $y = 0$ near to column 8, MEHMEL and WEISE show
that a reaction of 0.58 is to be expected in column 8 whereas the present method,
for the rectangular plate shown in Fig. 5, provides a value of 0.7128 with the

Fourier series truncated at $n = 60$. It is difficult to identify the precise reason for this large discrepancy, amounting to some 20 per cent, without a detailed knowledge of the experimental conditions, but it is unlikely that the difference in overhang at the ends has such a marked effect. For example, when the rectangular plate of Fig. 5 is shortened to $-1.0 \leq x \leq 1.0$ the present method provides the virtually identical value of 0.7127, moreover, the preliminary infinite plate solution itself provides a value of 0.7243 which represents a change of only 1.5 per cent. It is, however, extraordinarily difficult to measure accurately the reactions in a column supported plate because of the difficulty of aligning the supports in the plane of the plate and because the elasticity of the measuring device exerts its own influence on the distribution of the column reactions. We can form some estimate of these effects by referring to Table 4 which provides details, calculated by the present method, of the column reactions caused by unit settlement of various columns. Thus, in MEHMEL and WEISE's experiment the plate measures essentially $60 \,\mathrm{cm} \times 60 \,\mathrm{cm}$ with a thickness of $0.5 \,\mathrm{cm}$ and a Young's modulus of $753\,000 \,\mathrm{kg/cm^2}$ giving a flexural rigidity $D = 8270 \,\mathrm{kg\,cm}$. Table 4 now shows that a relative settlement or misalignment as small as $0.005 \,\mathrm{cm}$ (i. e. one hundredth of the plate thickness) at column 8 causes a reaction in that column of amount

$$\frac{-429.5 \times 0.005 \times 8270}{60 \times 60} = -4.9 \,\mathrm{kg}$$

and this is significant when it is noted that the individual support reactions are of the order of $15 \,\mathrm{kg}$ in the experiment.

9.2.1. Effect of Elastic Column Supports

In their experiments MEHMEL and WEISE [14] investigate also the effect which occurs when all the column supports have a finite and uniformly linear elasticity, they take N as the non-dimensional elasticity parameter where

$$N = \frac{w}{F} \frac{12 D (1 - \nu^2)}{4 b^2} \tag{9.1}$$

with w and F respectively as the individual column settlement and reaction and $2b$ as the width of the plate. As mentioned in the Introduction, the present method can be adapted to this case or the question can be dealt with by an auxiliary calculation in the manner described below.

Let us consider the specific example of a concentrated load of unit intensity applied directly over column 8 in Fig. 5. Table 4 provides the reactions caused by unit settlement of various columns and these are now interpreted as loads (i. e. sign reversed) applied to the plate so that there are no reactions except in the columns which suffer the unit settlement. To provide this unit settlement the column must suffer a reaction of amount F where

$$F = \frac{12 D (1 - \nu^2)}{4 b^2 N} \tag{9.2}$$

L. S. D. MORLEY

Table 4. Reactions caused by unit settlement of various columns in the rectangular plate shown in Fig. 5. Poisson's ratio $\nu = 0.228$

Column No.	Column reactions caused by unit settlement at		
	Columns 6 and 10	Columns 7 and 9	Column 8
1	$5.8\,D$	$-3.9\,D$	$-2.0\,D$
2	$-3.6\,D$	$2.6\,D$	$0.9\,D$
3	$-4.5\,D$	$2.5\,D$	$2.1\,D$
4	$-3.6\,D$	$2.6\,D$	$0.9\,D$
5	$5.8\,D$	$-3.9\,D$	$-2.0\,D$
6	$-80.5\,D$	$142.6\,D$	$-62.2\,D$
7	$143.6\,D$	$-420.5\,D$	$276.9\,D$
8	$-126.3\,D$	$555.7\,D$	$-429.5\,D$
9	$143.6\,D$	$-420.5\,D$	$276.9\,D$
10	$-80.5\,D$	$142.6\,D$	$-62.2\,D$

from Eq. (9.1), and this requires an addition to the loads quoted in Table 4. The first column in Table 4 now reads $-5.8\,D, 3.6\,D, 4.5\,D, 3.6\,D, -5.8\,D, 80.5\,D + F,$ $-143.6\,D, 126.3\,D, -143.6\,D, 80.5\,D + F$ and this is regarded as a principal force group and is denoted by $F_{6,10}$. In the same way we form principal force groups $F_{7,9}$, F_8 and, by symmetry the force groups $F_{1,5}$, $F_{2,4}$ and F_3. These principal force groups may be combined so that

$$F^* = C_{1,5} F_{1,5} + C_{2,4} F_{2,4} + C_3 F_3 + C_{6,10} F_{6,10} + C_{7,9} F_{7,9} + C_8 F_8, \qquad (9.3)$$

where F^* represents the actual applied loading condition, i. e. a unit concentrated load applied directly over column 8. The values of the constants $C_{1,5}$, $C_{2,4}$, etc. are determined from the following set of simultaneous equations which equate the loads in turn as column positions $1, 5, 2, 4$, etc.

$$\begin{bmatrix} 80.5 + F/D & -142.6 & 62.2 & -5.8 & 3.9 & 2.0 \\ -143.6 & 420.5 + F/D & -276.9 & 3.6 & -2.6 & -0.9 \\ 126.3 & -555.7 & 429.5 + F/D & 4.5 & -2.5 & -2.1 \\ -5.8 & 3.9 & 2.0 & 80.5 + F/D & -142.6 & 62.2 \\ 3.6 & -2.6 & -0.9 & -143.6 & 420.5 + F/D & -276.9 \\ 4.5 & -2.5 & -2.1 & 126.3 & -555.7 & 429.5 + F/D \end{bmatrix} \begin{bmatrix} C_{1,5} \\ C_{2,4} \\ C_3 \\ C_{6,10} \\ C_{7,9} \\ C_8 \end{bmatrix} = \begin{bmatrix} 0 \\ 0 \\ 0 \\ 0 \\ 0 \\ 1/D \end{bmatrix}. \qquad (9.4)$$

The resulting column reactions are simply $F\,C_{1,5}$ in columns 1 and 5, $F\,C_{2,4}$ in columns 2 and 4, etc. where F is as given by Eq. (9.2).

MEHMEL and WEISE find for a value of $N = 0.8$ that the reaction in column 8 is 0.31 whereas the above calculation provides a reaction of 0.258. Again, it is difficult to explain this fairly large discrepancy without a detailed knowledge of the experimental conditions. The variation of the reaction in column 8 with the column elasticity parameter is shown in Fig. 6 and this demonstrates very clearly the difficulty in simulating the rigid support condition, $N = 0$, in a model test; for N as small as 0.001 the reaction in column 8 is reduced to 0.776.
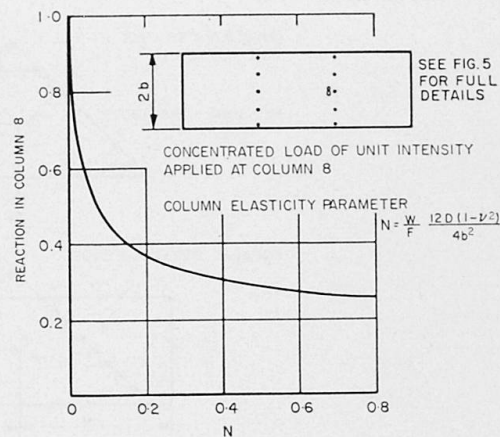

Fig. 6. Effect of elastic column supports on the reaction in a loaded column.

9.3. The Skew Plate

The arrangement of the column supports in a large proportion of bridge decks and elevated roadways is such that there is a marked degree of skewness and this has seriously complicated the design procedure. The importance of the problem has, however, led to a number of tabulations of design data for single span bridges which are derived either as the result of finite difference calculations on plates with continuously supported edges [11, 12] or from experiments on small scale models [3] which may be supported on discrete columns [14]. It is the present purpose to provide comparisons between the results obtained by the present method and typical results taken from these various tabulations. It must be borne in mind, however, that both the finite difference and experimental techniques are susceptible to inaccuracies of one kind or the other and comparisons between the various tabulations are complicated by the different values which are taken for the Poisson's ratio and by the different geometrical shapes. Moreover, the present representation of a skew plate by a rectangular plate means that there can be a considerable overhang, see Figs. 7, 8, 9 and 11, of irregular shape from the lines of support. This overhang provides a small amount of restraint and tends to reduce the general level of the bending moments in the plate. It is unfortunate that unlike the rigorous analysis of the rectangular plate by KURATA and OKAMURA [13] there is not available a similar treatment for these skew plates with which to establish even a few results for

plates with continuously supported edges with sufficient precision to provide a standard for comparison.

9.3.1. Rhombic Plate with 45° Skew

A single span rhombic plate with 45° skew under central concentrated load is shown in Fig. 7 where the two continuously supported edges as considered by ROBINSON [11] are each approximated here by seven equally spaced columns. ROBINSON examined the problem both by a finite difference analysis with the plate divided into 48 elemental parallelograms and also by experiment on a mild steel plate.
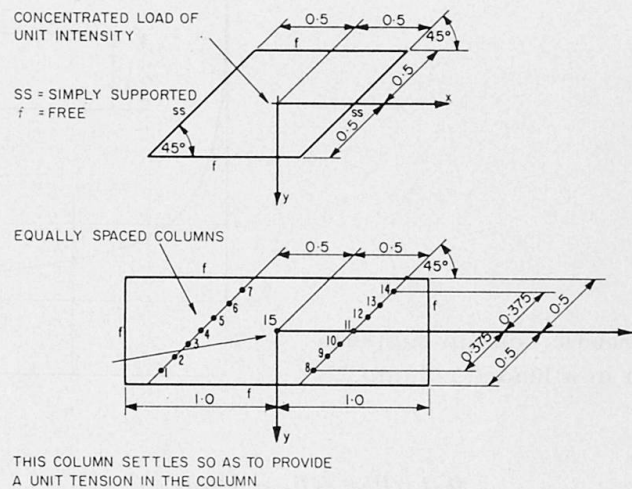

Fig. 7. Representation of a 45° skew rhombic plate with two opposite edges simply supported and other edges free, under central concentrated load.

The unit central concentrated load is simulated here by an additional central column number 15, see Fig. 7, which is allowed to settle just enough to produce a unit tension load in that column. The Fourier series of Eq. (7.1) is now truncated after $n = 80$ and Poisson's ratio is taken as $\nu = 0.3$ in agreement with Robinson's value. Table 5 provides comparative values of the deflection w

Table 5. Deflection w under unit central load in a 45° skew rhombic plate with two opposite edges simply supported, remaining edges free

Source	Poisson's ratio ν	w (theory)	w (experiment)
ROBINSON [11] (48 parallelograms)	0.3	0.0117/D	0.0099/D
Present (see Fig. 7)	0.3	0.01113/D	—

underneath the central load and it is seen that the present result is straddled by Robinson's theoretical and experimental results by the respective amounts of 5 and −10 per cent. The moments M_x, M_y and M_{xy} are listed in Table 6 for

Table 6. Moments M_x, M_y and M_{xy} in a 45° skew rhombic plate with unit central load and two opposite edges simply supported, remaining edges free. Comparison with Robinson's results, Poisson's ratio $v = 0.3$

Co-ordinate position (see Fig. 7)		M_x		M_y		M_{xy}	
x	y	Robinson [11] (48 parallelograms)	Present (see Fig. 7)	Robinson [11] (48 parallelograms)	Present (see Fig. 7)	Robinson [11] (48 parallelograms)	Present (see Fig. 7)
0.167	0	0.083	0.0840	0.128	0.1190	0.044	0.0492
0.333	0	0.011	0.0175	0.051	0.0540	0.023	0.0235
0.088	−0.088	0.164	0.1568	0.131	0.1177	0.083	0.0828
0.177	−0.177	0.106 (0.112)	0.1045	0.061 (0.069)	0.0539	0.069 (0.073)	0.0666
0.265	−0.265	0.080	0.0813	0.024	0.0222	0.050	0.0487
0.354	−0.354	0.060 (0.062 *)	0.0647	0	0.0000	0.032 (0.039 *)	0.0323

The results in parentheses are obtained from experiment by Rüsch and Hergenröder [3] on a model with Poisson's ratio $v = 0.215$.
* Indicates that the result is appropriate to the co-ordinate position $x = 0.325$, $y = -0.325$.

Table 8. Moments M_x, M_y and M_{xy} in a 60° skew rhombic plate with unit central load and two opposite edges simply supported, remaining edges free. Comparison with Balas and Hanuska's results, Poisson's ratio $v = 0.1667$

Co-ordinate position (see Fig. 8)		M_x		M_y		M_{xy}	
x	y	Balas and Hanuska [12]	Present (see Fig. 8)	Balas and Hanuska [12]	Present (see Fig. 8)	Balas and Hanuska [12]	Present (see Fig. 8)
0.125	0	0.049	0.0413 (0.0413)	0.149	0.1311 (0.1310)	0.029	0.0469 (0.0467)
0.250	0	−0.005	0.0003 (0.0001)	0.080	0.0668 (0.0668)	0.010	0.0214 (0.0211)
0.375	0	−0.011	−0.0051 (−0.0056)	0.041	0.0341 (0.0341)	−0.003	0.0058 (0.0054)
0.144	−0.088	0.053	0.0084 (0.0084)	0.092	0.0869 (0.0869)	0.058	0.0093 (0.0092)
0.288	−0.166	0.018	−0.0179 (−0.0183)	0.030	0.0138 (0.0138)	0.038	−0.0170 (−0.0173)
0.433	−0.250	0.005	−0.0019 (−0.0024)	0	0.0000 (0.0000)	0.016	−0.0097 (−0.0102)

The results in parentheses are appropriate to a truncation of the Fourier series after $n = 80$.

stations midway between the free edges and also midway between the simply supported edges, the maximum listed value differing this time by only some 4 per cent from Robinson's. The results in parentheses in Table 6 are obtained from the experimental work of RÜSCH and HERGENRÖDER on plaster models having a Poisson's ratio $\nu = 0.215$, they are generally larger than both those of ROBINSON and the present method where $\nu = 0.3$.

9.3.2. Rhombic Plate with 60° Skew (10 Column Supports)

An angle of skew greater than 60° is rarely encountered in practice and so this generally forms the limiting, and most difficult, case for which data is tabulated [2, 3, 11, 12, 14]. The problem of a single span rhombic plate is now examined in detail which, in the first instance, is approximated by a rectangular plate with each of the supported edges resting upon five equally spaced columns as shown in Fig. 8. A central concentrated load of unit intensity at $x = 0$, $y = 0$ is again
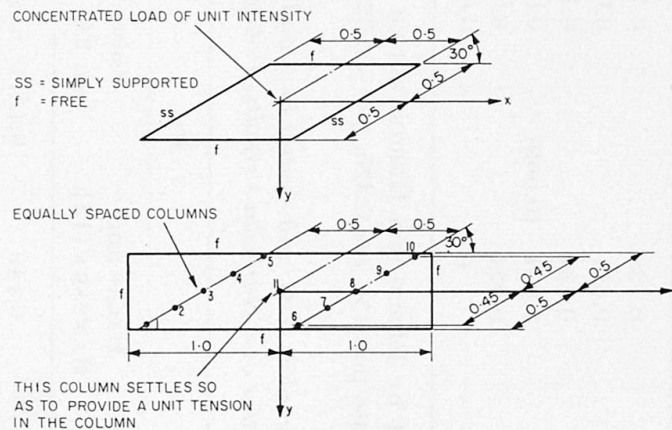

Fig. 8. Representation of a 60° skew rhombic plate with two opposite edges simply supported and other edges free, under central concentrated load.

simulated by a central column, number 11, which is allowed to settle just enough to produce a unit tension load in the column. The Fourier series of Eq. (7.1) is truncated after $n = 60$ and the two values of Poisson's ratio $\nu = 0.1667$ and $\nu = 0.228$ are considered. This enables a comparison of results for both the central deflection, see Table 7, and the moments, see Table 8, to be obtained for the plate with continuously supported edges as considered in the finite differ-

Table 7. *Deflection w under unit central load in a 60° skew rhombic plate with two opposite edges simply supported, remaining edges free*

Source	Poisson's ratio ν	Central deflection w
BALAS and HANUSKA [12] (48 parallelograms)	0.1667	0.00555/D
Present (see Fig. 8)	0.1667	0.005173/D

ence analysis of BALAS and HANUSKA [12] for Poisson's ratio $\nu = 0.1667$, along with a comparison of the column reactions, see Table 9, obtained by MEHMEL and WEISE [14] in their experiments on a plate glass model with Poisson's ratio $\nu = 0.228$.

Table 9. Column reaction caused by unit central load in a 60° skew rhombic plate with column supports arranged as shown in Fig. 8. Poisson's ratio $\nu = 0.228$

Column Nos.	Column reactions	
	MEHMEL and WEISE [14]	Present
1, 10	—	0.0009
2, 9	—	− 0.0043
3, 8	—	0.0001
4, 7	0.06	0.0672
5, 6	0.42	0.4362

Table 7 shows that BALAS and HANUSKA calculate a value for the central deflection which is about 7 per cent larger than that obtained from the present method and this exhibits the same trend as for their square plate results in Table 1 where the percentage difference is nearly the same. The maximum moment listed in Table 8 is a value for M_y and there is a disagreement here of some 14 per cent from the larger value calculated by BALAS and HANUSKA which repeats more markedly the trend exhibited by M_y for the square plate, see Table 3. This disparity between the two sets of results is attributed to the relatively coarse mesh of 48 elemental parallelograms which BALAS and HANUSKA use for their finite difference calculation. As a check, the present calculations were repeated with an increased number of terms in the Fourier series, now truncated after $n = 80$. These results are shown in parentheses in Table 8 and there is seen to be little change of significance in the values of the moments.

Table 9 lists the column reactions and it is seen that the unit load is reacted almost entirely by the columns at the obtuse corners, i. e. numbers 5 and 6. Unlike the comparison of column reactions for the square plate in Section 9.2 there is agreement here to within 3.7 per cent of the smaller value obtained by MEHMEL and WEISE in their experiment and which is consistent with an alleviation produced by a slight column elasticity or settlement.

9.3.3. Rhombic Plate with 60° Skew (24 Column Supports)

The purpose of this second examination of a 60° skew rhombic plate is to obtain a comparison with the results measured by ANDRÄ and LEONHARDT [2] in their experiments on column supported aluminium plates with Poisson's ratio $\nu = 0.33$ and with the extensive work of RÜSCH and HERGENRÖDER [3] in their experiments on plaster models with continuously supported edges where $\nu =$

0.215. For the present examination the plate is supported upon 24 columns as shown in Fig. 9 and the moments in the plate are calculated at the locations, I, II and III which are used as control positions by ANDRÄ and LEONHARDT and at A, B ($\equiv$III), C, D, E and E_2 to correspond with the control positions of RÜSCH and HERGENRÖDER. For these calculations the Fourier series of Eq. (7.1) is truncated after $n = 80$ and two positions are considered for the concentrated load which is again of unit intensity.
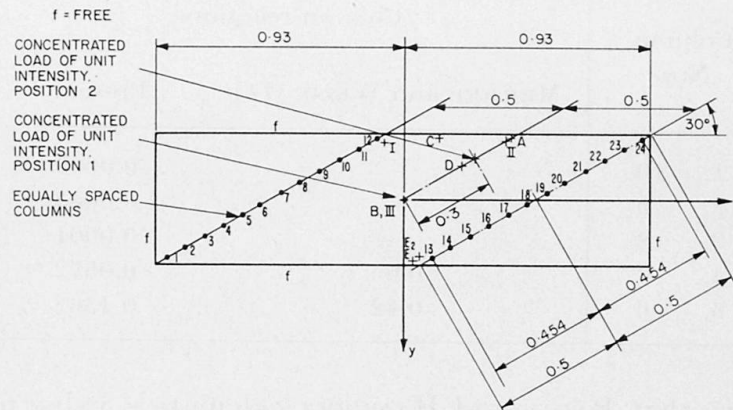

Fig. 9. Representation of a 60° skew rhombic plate supported on 24 columns and under concentrated load.

The concentrated load is first situated at the centre of the plate and the resulting column reactions, for $\nu = 0.33$, are listed in Table 10. Again, the applied load is reacted almost entirely by the columns located at the obtuse corners, numbers 12 and 13. The value of this reaction as measured by ANDRÄ and LEONHARDT is nearly 10 per cent smaller than that obtained by the present method and this is again consistent with an alleviation produced by a slight column elasticity or settlement.

The concentrated load is now moved to position 2, see Fig. 9, in order to secure a more significant comparison with the bending and twisting moments which were measured in the experiments. The column reactions for this loading case are listed in Table 10 and it is noted that, for $\nu = 0.33$, the maximum value is now 1.257 times the magnitude of the applied load and the value measured by ANDRÄ and LEONHARDT is nearly 6 per cent smaller than this. The adjacent column suffers a large tension of -0.775 times the magnitude of the applied load. The results in parentheses are for Poisson's ratio $\nu = 0.215$.

The values of the bending and twisting moments are listed in Table 11 where ANDRÄ and LEONHARDT's results are derived by interpolating from their illustrations of the influence curves and, along with RÜSCH and HERGENRÖDER's results, are resolved where necessary so that the directions of the moments correspond with those of the present paper. It was necessary to reverse the sign of the twisting moment as given by RÜSCH and HERGENRÖDER. The comparison between the values is disappointing. Following the trend exhibited in Section

Table 10. Column reactions caused by unit load in a 60° skew rhombic plate with column supports arranged as shown in Fig. 9. Poisson's ratio ν = 0.33

Column Nos.	Column reactions			
	Load at position 1		Load at position 2	
	ANDRÄ and LEONHARDT [2]	Present	ANDRÄ and LEONHARDT [2]	Present
1	—	− 0.0011	—	0.003 (0.002)
2	—	0.0054	—	0.001 (0.000)
3	—	0.0005	—	0.000 (− 0.001)
4	—	− 0.0003	—	− 0.002 (− 0.003)
5	—	− 0.0013	—	− 0.005 (− 0.006)
6	—	− 0.0013	—	− 0.008 (− 0.008)
7	—	0.0009	—	− 0.011 (− 0.011)
8	—	0.0090	—	− 0.011 (− 0.011)
9	—	0.0231	—	− 0.034 (− 0.033)
10	—	0.0990	—	0.085 (0.077)
11	− 0.07	− 0.1004	− 0.66	− 0.775 (− 0.745)
12	0.42	0.4665	1.19	1.257 (1.239)
13	0.42	0.4665	0.00	− 0.015 (− 0.049)
14	− 0.08	− 0.1004	− 0.18	− 0.069 (− 0.045)
15	—	0.0990	—	− 0.006 (0.004)
16	—	0.0231	—	0.087 (0.099)
17	—	0.0090	—	0.160 (0.167)
18	—	0.0009	—	0.152 (0.153)
19	—	− 0.0013	—	0.104 (0.100)
20	—	− 0.0013	—	0.063 (0.055)
21	—	− 0.0003	—	0.033 (0.025)
22	—	0.0005	—	0.009 (0.005)
23	—	0.0054	—	0.016 (0.013)
24	—	− 0.0011	—	− 0.035 (− 0.028)

The results in parentheses are for Poisson's ratio ν = 0.215.

9.3.1, RÜSCH and HERGENRÖDER's results are generally larger, sometimes by as much as 25 per cent, than the results calculated by the present method. The absolute magnitude of ANDRÄ and LEONHARDT's most significant result is some 14 per cent smaller than the present value. To try and resolve these discrepancies the moments M_x, M_y and M_{xy} were plotted as shown in Fig. 10 for a section passing through the control points B, D and A (see Fig. 9) and also for a section passing through the control points C and A. It is seen that many of RÜSCH and HERGENRÖDER's results lie in regions of rapidly varying stress and, in consequence, the comparison of results as depicted by Fig. 10 is moderately good except for the value of M_{xy} at control point C. It should be noted that RÜSCH and HERGENRÖDER derive their moments from strain gauge rosettes located a slight

Table 11. Comparison of moments M_x, M_y and M_{xy} in a 60° skew rhombic plate under a concentrated load of unit intensity at position 2, see Fig. 9

Loca-tion	Co-ordinate position (see Fig. 9)		M_x				M_y				M_{xy}			
	x	y	Rüsch and Hergenröder [3] $\nu = 0.215$	Andrä and Leonhardt [2] $\nu = 0.33$	Present (see Fig. 9) $\nu = 0.215$	Present (see Fig. 9) $\nu = 0.33$	Rüsch and Hergenröder [3] $\nu = 0.215$	Andrä and Leonhardt [2] $\nu = 0.33$	Present (see Fig. 9) $\nu = 0.215$	Present (see Fig. 9) $\nu = 0.33$	Rüsch and Hergenröder [3] $\nu = 0.215$	Andrä and Leonhardt [2] $\nu = 0.33$	Present (see Fig. 9) $\nu = 0.215$	Present (see Fig. 9) $\nu = 0.33$
I	−0.067	−0.208	—	−0.267	−0.2920	−0.3051	—	−0.010	−0.0242	−0.0317	—	−0.151	−0.1464	−0.1425
II	0.385	−0.222	—	0.203	0.1790	0.1931	—	0.022	0.0229	0.0224	—	−0.040	−0.0456	−0.0358
III, B	0	0	−0.003	−0.004	−0.0002	0.0055	0.047	0.032	0.0466	0.0461	−0.101	−0.098	−0.0979	−0.0914
A	0.398	−0.230	0.198	—	0.1633	0.1765	—	—	0.0152	0.0145	−0.047	—	−0.0385	−0.0281
C	0.138	−0.230	0.188	—	0.1616	0.1702	—	—	0.0168	0.1756	−0.197	—	−0.1461	−0.1528
D	0.217	−0.125	0.287	—	0.2667	0.2843	0.149	—	0.1241	0.1383	−0.149	—	−0.1412	−0.1321
E	0.038	0.235	0.067	—	0.0696	0.0677	−0.014	—	0.0027	0.0026	−0.037	—	−0.0587	−0.0546
E_2	0.056	0.208	0.060	—	0.0758	0.0732	−0.016	—	0.0055	0.0062	−0.038	—	−0.0628	−0.0591

distance away from the reference point (ANDRÄ and LEONHARDT measure the curvatures of the plate). Also, the overhang of the rectangular plate at the lines of support, see Fig. 9, provides a small amount of restraint which tends to reduce the general level of bending moments as calculated by the present method.

Fig. 10 shows clearly the logarithmic singularity which occurs in the values of M_x and M_y at the concentrated load position. The rational interpretation of this singularity in practice must take proper account of the two dimensional nature of the actual loading distribution and the three dimensional character of the stress distribution in that region.
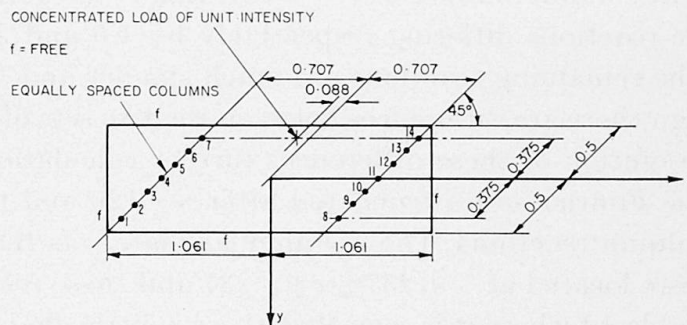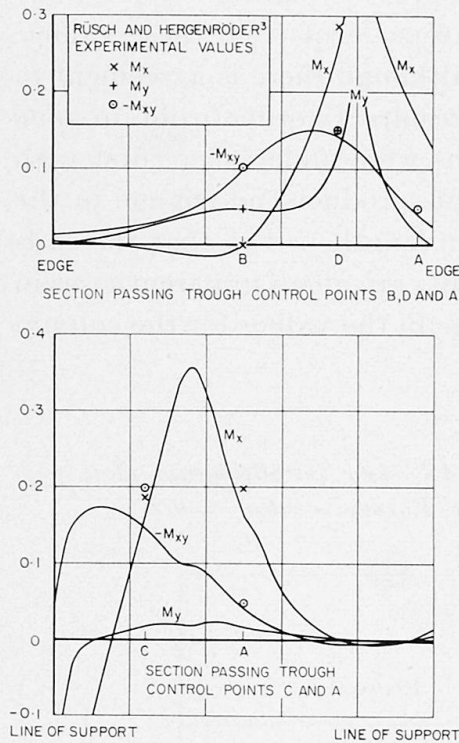

Fig. 11. Representation of a 45° skew parallelogram plate supported on 14 columns and under a concentrated load.

Fig. 10. Distribution of the moments across two sections of the plate shown in Fig. 9 with the unit concentrated load at position 2.

9.3.4. Parallelogram Plate with 45° Skew

The column reactions in a parallelogram plate with 45° skew under unit concentrated load and supported on 14 columns, as shown in Fig. 11, are now determined in order to obtain a comparison with the results of the computer program developed by JEAN-CLAUDE LERAY [6] following the analysis of JEAN LERAY [7, 8]. This analysis proceeds from the biharmonic Green's function, determined through numerical quadrature, for the behaviour of an infinitely long strip with free edges and supported at infinity. The computations are restricted in so far as the locations of the column supports and applied loads must coincide with the nodes of a square network which generally divides the width of the strip into 10 equal parts, although a finer network with 14 equal parts across the width can also be considered; no allowance is made for the finite length of the plate. These limitations do not permit the accuracy of the numerical results to be

investigated by advancing to a finer network (cf. the ease of increasing the number of terms in the Fourier series for the present method) or by modifying the length of the plate. Nevertheless, the work of LERAY provides the basis for a remarkable set of calculations which overcome many of the difficulties which are mentioned in the present Introduction.

The results of the calculations for the column reactions are listed in Table 12 where Poisson's ratio is taken as $\nu = 0.2$ to correspond with that of LERAY. The Fourier series of Eq. (7.1) is truncated after $n = 100$. It is interesting to note that although the load is only of unit intensity the reaction in column number 7, at the prominent obtuse corner, is 1.634 and there is a large tension in the adjacent column number 6 of -0.974. LERAY's results provide slightly less pessimistic reactions differing respectively by 1.5 and 3.6 per cent from these values. The remaining reactions are much smaller and, although there is agreement in sign there are differences between the two sets of results. In order to obtain some resolution of these differences further calculations were undertaken, first with the Fourier series truncated after $n = 120$ and this produces no change in the column reactions. The rectangular plate was then lengthened so that the ends were located at $-1.237 \leqq x \leqq 1.237$ and these results are given in parentheses in Table 12 where it is seen that there is little change in the values for the column reactions.

Table 12. *Column reactions caused by unit load in a 45° skew parallelogram plate with column supports arranged as shown in Fig. 11. Poisson's ratio $\nu = 0.2$*

Column Nos.	Column reactions	
	LERAY [6]	Present
1	0.022	0.064 (0.053)
2	-0.067	-0.097 (-0.082)
3	-0.036	-0.034 (-0.035)
4	-0.061	-0.063 (-0.063)
5	0.033	0.032 (0.031)
6	-0.939	-0.974 (-0.976)
7	1.61	1.634 (1.635)
8	-0.051	-0.003 (-0.004)
9	0.144	0.069 (0.070)
10	0.111	0.102 (0.102)
11	0.108	0.108 (0.108)
12	0.076	0.088 (0.088)
13	0.068	0.096 (0.096)
14	-0.018	-0.023 (-0.023)

The results in parentheses are for a longer plate with the ends located at $-1.237 \leqq x \leqq 1.237$, see Fig. 11.

9.4. Model of the Cumberland Basin Elevated Road System

In the absence of an adequate method of theoretical analysis BEST and WEST [1] obtained basic design data by testing a $^1/_{24}$ th scale model of a part of the system of elevated roadways for the Cumberland Basin in Bristol. The actual structure is a reinforced concrete slab supported on columns and is of uniform thickness (24 inches) except for edge beams. The columns are generally arranged in lines of three, symmetrically disposed across the width of the slab but, at one point, the elevated slab crosses over a road at a considerable angle of skew and this requires a rearrangement of the columns to provide one skewed parallelogram span directly over the lower road and two trapezoidal spans, one on either side of the centre, before the columns are again arranged in lines perpendicular to the line of the road.

For their model representation, BEST and WEST made a rectangular slab from micro-concrete of uniform one inch thickness measuring 120 inches by 27 inches and supported upon 20 columns. For the present representation, see Fig. 12, the plate measures 130 inches by 27 inches and values of the flexural
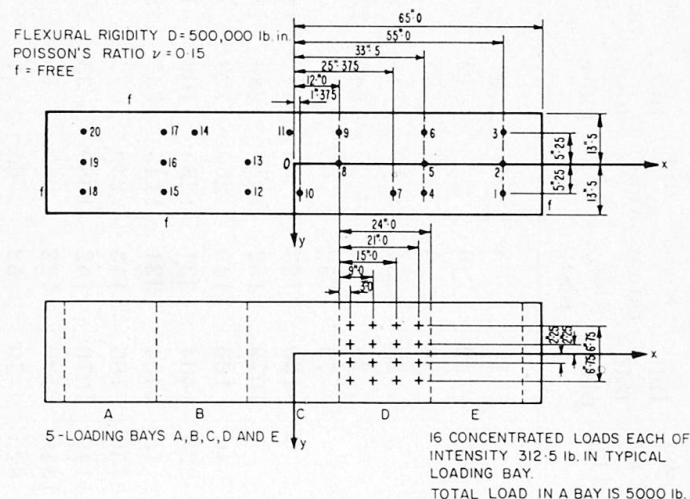

Fig. 12. Representation of the model of the Cumberland Basin elevated road system.

rigidity $D = 500\,000$ lb in and Poisson's ratio $v = 0.15$ are assumed. Five loading cases are considered which consist of a group of sixteen concentrated loads acting respectively in the loading bays A, B, C, D and E as shown in Fig. 12 with the Fourier series of Eq. (7.1) truncated after $n = 80$. Three sets of column reactions are listed in Table 13 for each loading case, they consist of the reactions as calculated from the preliminary infinite plate solution, the reactions calculated for the rectangular plate as depicted in Fig. 12 and the reactions measured by BEST and WEST.

There is reasonable agreement with the measured results although it is noted that there is a general tendency for the measured values to be optimistic and this is consistent with the presence, in the experiment, of elasticity in the supports

Table 13. *Column reactions caused by loads applied respectively in bays A, B, C, D and E of the model of the Cumberland Basin elevated road system. Poisson's ratio ν = 0.15*

Column No.	Loads applied in bay A			Loads applied in bay B			Loads applied in bay C			Loads applied in bay D			Loads applied in bay E			Sum of A, B, C, D and E		
	Present		BEST and WEST [1]	Present		BEST and WEST [1]	Present		BEST and WEST [1]	Present		BEST and WEST [1]	Present		BEST and WEST [1]	Present		BEST and WEST [1]
	Infinite plate	Rectangular plate		Infinite plate	Rectangular plate		Infinite plate	Rectangular plate		Infinite plate	Rectangular plate		Infinite plate	Rectangular plate		Infinite plate	Rectangular plate	
1	8	0	—	−1	0	—	−11	−5	—	−31	−2	20	701	710	765	666	703	785
2	−5	0	—	5	1	—	22	6	—	−12	−1	20	1721	1598	1410	1731	1604	1430
3	11	0	—	−6	0	—	−4	6	—	−83	−90	−80	719	752	770	637	668	690
4	−7	0	—	−4	−7	—	29	54	10	−145	−217	0	933	1037	975	806	867	985
5	3	2	—	2	−9	—	24	−15	−25	1285	1376	1185	970	1060	875	2284	2414	2035
6	−4	2	—	−4	0	—	−79	−52	−65	803	752	775	571	580	545	1287	1282	1255
7	−2	−2	—	16	29	5	−130	−123	−50	1497	1443	1365	−521	−620	−435	860	727	885
8	−1	−17	—	33	31	−5	1079	1152	1060	1283	1350	1220	2	−3	−95	2396	2513	2180
9	−5	−9	—	−2	3	−40	166	145	260	729	729	745	−166	−209	−125	722	659	840
10	33	59	70	−257	−285	−225	1404	1331	1235	−106	−100	−15	41	61	35	1115	1066	1100
11	41	61	70	−106	−100	−15	1404	1331	1145	−257	−285	−180	33	59	35	1115	1066	1055
12	−166	−209	−140	729	729	750	166	145	230	−2	3	−15	−5	−9	—	722	659	825
13	2	−3	−130	1283	1350	1140	1079	1152	1080	33	31	−15	−1	−17	—	2396	2513	2075
14	−521	−620	−365	1497	1443	1340	−130	−123	−55	16	29	15	−2	−2	—	860	727	935
15	571	580	600	803	752	825	−79	−52	−65	−4	0	—	−4	2	—	1287	1282	1360
16	970	1060	910	1285	1376	1120	24	−15	−5	2	−9	—	3	0	—	2284	2414	2025
17	933	1037	930	−145	−217	20	29	54	5	−4	−7	—	−7	0	—	806	867	955
18	719	752	770	−83	−90	−95	−4	6	—	−6	0	—	11	0	—	637	668	675
19	1721	1598	1495	−12	−1	0	22	6	—	5	1	—	−5	0	—	1731	1604	1495
20	701	710	775	−31	−2	−25	−11	−5	—	−1	0	—	8	0	—	666	703	750

N.B. All loads are in lb. Total load in a bay is 5000 lb.

(i. e. in the load measuring devices). In particular, for the five loading cases in bays A, B, C, D and E the maximum column reaction as calculated by the present method for the rectangular plate is respectively some 7, 8, 8, 6 and 13 per cent larger than the measured value. The sum of the five loading cases gives an approximation to a uniformly distributed load and the present method provides a maximum column reaction for the rectangular plate which is some 15 per cent larger than that measured by Best and West. In order to examine the accuracy of the results the calculations for the loading case in bay B were repeated with the Fourier series truncated after $n = 130$ and it was found that there was no change in any of the column reactions listed in Table 13.

The calculations for the present method commence with the preliminary infinite plate solution which is, in itself, a fairly trivial calculation. The results of this preliminary infinite plate solution are recorded in the Table because they are seen to provide, in this instance, a good approximation to the actual column reactions. In fact, for the five loading cases in bays A, B, C, D and E the maxi-

Table 14. Column reactions caused by 0.005 in settlement at columns 5 and 8 in the model of the Cumberland Basin elevated road system. Poisson's ratio $v = 0.15$, flexural rigidity $D = 500000$ lb. in.

Column No.	0.005 in settlement at column 5		0.005 in settlement at column 8	
	Infinite plate	Rectangular plate	Infinite plate	Rectangular plate
1	− 48	− 33	− 6	0
2	87	80	13	4
3	− 49	− 35	− 12	− 3
4	333	278	− 80	− 80
5	− 694	− 608	50	54
6	357	293	− 37	− 29
7	19	10	165	151
8	50	54	− 513	− 448
9	− 27	− 19	293	233
10	− 30	− 23	184	159
11	− 8	− 3	− 16	− 12
12	− 4	4	− 53	− 50
13	16	4	19	24
14	− 5	− 1	− 15	− 9
15	− 5	− 1	− 4	3
16	8	0	16	4
17	− 3	0	− 5	1
18	− 2	− 1	− 3	− 1
19	4	1	6	2
20	− 2	− 1	− 5	− 1

N.B. All loads are in lb.

mum column reactions are predicted to within accuracies of 8, 0.5, 6, 0.5 and 8 per cent respectively, while for the sum of the loading cases the maximum column reaction is predicted to within -5 per cent. These values lie within the bounds of normal experimental error and it follows, moreover, that in this model the column reactions are virtually independent of Poisson's ratio.

The most heavily loaded columns for the sum of the loading cases are columns $5 (\equiv 16)$ and $8 (\equiv 13)$ and it is of interest to examine the effect of relative settlement at these positions. The column reactions resulting from a 0.005 inch settlement of these columns are recorded in Table 14 where it is seen that this modest settlement causes as much as 25 per cent change in the value of the maximum column reaction and this emphasizes, once again, the grave difficulties which have to be surmounted in experimental work on column supported plates. The Table shows also that the preliminary infinite plate solution again provides a reasonable estimate of the column reactions for this model.

Appendix A
The Singular Solution for the Orthotropic Plate

In order to extend the aforegoing analysis to the problem of the orthotropic plate it is necessary to have available the singular solution of the governing partial differential equation

$$D_x \frac{\partial^4 w}{\partial x^4} + 2 H \frac{\partial^4 w}{\partial x^2 \partial y^2} + D_y \frac{\partial^4 w}{\partial y^4} = 0 \tag{A.1}$$

appropriate to a concentrated force of unit intensity acting at the origin of coordinates in a plate of infinite extent. The fundamental equations for orthotropic plates are given in the book by TIMOSHENKO and WOINOWSKY-KRIEGER [5]; in Eq. (A.1) D_x and D_y are the flexural rigidities in the x and y directions respectively while H includes the plate shear rigidity together with a coupling rigidity arising from the Poisson ratio effect.

It is convenient to introduce the notation

$$\lambda = \left(\frac{D_x}{D_y}\right)^{1/4}, \qquad \mu = \frac{H}{(D_x D_y)^{1/2}}, \tag{A.2}$$

so that the general solution to Eq. (A.1) may be written

$$w(x, y) = F_1(x + \gamma y) + F_2(x + \bar{\gamma} y) + F_3(x - \gamma y) + F_4(x - \bar{\gamma} y), \tag{A.3}$$

where γ is root of the characteristic equation

$$\gamma^4 + 2 \mu \gamma^2 \lambda^2 + \lambda^4 = 0 \tag{A.4}$$

and $\bar{\gamma}$ is the complex conjugate of γ. The required root of Eq. (A.4) is

$$\gamma = \frac{\lambda}{\sqrt{2}} \{(1-\mu)^{1/2} + i\,(1+\mu)^{1/2}\},$$

$$= \gamma_1 + i\,\gamma_2 \quad \text{say,}$$

(A.5)

where $i = \sqrt{-1}$. The singular solution of Eq. (4.1) for the case of isotropy suggests, in conjunction with Eq. (A.3), that we consider the singular solution

$$w\,(x,y) = C\,\{\bar{\gamma}\,(x+\gamma\,y)^2 \log\,(x+\gamma\,y)^2 + \gamma\,(x+\bar{\gamma}\,y)^2 \log\,(x+\bar{\gamma}\,y)^2$$
$$+ \bar{\gamma}\,(x-\gamma\,y)^2 \log\,(x-\gamma\,y)^2 + \gamma\,(x-\bar{\gamma}\,y)^2 \log\,(x-\bar{\gamma}\,y)\},$$

(A.6)

where C is a constant, the value of which is determined later. It is necessary to pay careful attention to the value of $\log\,(x+\gamma\,y)^2$ which is a multi-valued function for, on using Eq. (A.5),

$$\log\,(x+\gamma\,y)^2 = \log\,\{(x+\gamma_1\,y) + i\,\gamma_2\,y\}^2,$$

$$= \log\,\{(x+\gamma_1\,y)^2 + \gamma_2^2\,y^2\} + 2\,i\,\tan^{-1}\frac{\gamma_2\,y}{x+\gamma_1\,y}.$$
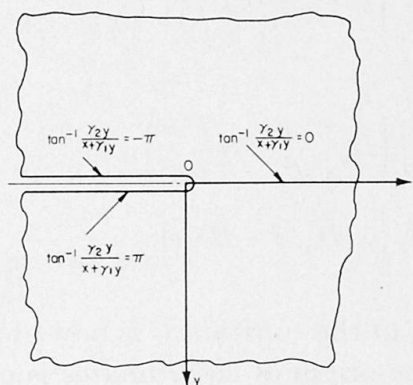
(A.7)

Fig. 13. Convention for the multi-valued function $\tan^{-1}\dfrac{\gamma_2\,y}{x+\gamma_1\,y}$.

The convention for the multi-valued part is illustrated in Fig. 13. Thus, for $x < 0$ and $y = +0$

$$\log\,(x+\gamma\,y)^2 = 2\log x + 2\,i\,\pi; \qquad \log\,(x+\bar{\gamma}\,y)^2 = 2\log x - 2\,i\,\pi;$$
$$\log\,(x-\gamma\,y)^2 = 2\log x - 2\,i\,\pi; \qquad \log\,(x-\bar{\gamma}\,y)^2 = 2\log x + 2\,i\,\pi;$$

(A.8a)

and similarly for $x < 0$ and $y = -0$

$$\log\,(x+\gamma\,y)^2 = 2\log x - 2\,i\,\pi; \qquad \log\,(x+\bar{\gamma}\,y)^2 = 2\log x + 2\,i\,\pi;$$
$$\log\,(x-\gamma\,y)^2 = 2\log x + 2\,i\,\pi; \qquad \log\,(x-\bar{\gamma}\,y)^2 = 2\log x - 2\,i\,\pi.$$

(A.8b)

The solution of Eq. (A.6) must conform with certain conditions. The solution is obviously real and the constant C can be adjusted to correspond with a concentrated load of unit intensity at the origin of co-ordinates but, in view of Eq. (A.7), it is necessary also that w and its first four derivatives with respect to y be continuous across the line $y = 0$. Since

$$w\,(x,y) = w\,(x,-y)$$

(A.9)

the continuity of w, $\partial^2 w/\partial y^2$ and $\partial^4 w/\partial y^4$ is assured. Furthermore,

$$\frac{\partial w}{\partial y} = 2\,C\,\gamma\,\bar{\gamma}\,\{(x+\gamma\,y)\log(x+\gamma\,y)^2 + (x+\gamma\,y) + (x+\bar{\gamma}\,y)\log(x+\bar{\gamma}\,y)^2 + (x+\bar{\gamma}\,y)$$
$$- (x-\gamma\,y)\log(x-\gamma\,y)^2 - (x-\gamma\,y) - (x-\bar{\gamma}\,y)\log(x-\bar{\gamma}\,y)^2 - (x-\bar{\gamma}\,y)\}$$

$$(A.10)$$

and from Eqs. (A.8a) it is seen for $x<0$ and $y=+0$ that $\partial w/\partial y=0$ as is required. The third derivative is

$$\frac{\partial^3 w}{\partial y^3} = 4\,C\,\gamma\,\bar{\gamma}\left\{\frac{\gamma^2}{x+\gamma\,y} + \frac{\bar{\gamma}^2}{x+\bar{\gamma}\,y} - \frac{\gamma^2}{x-\gamma\,y} - \frac{\bar{\gamma}^2}{x-\bar{\gamma}\,y}\right\} \qquad (A.11)$$

and clearly $\partial^3 w/\partial y^3 = 0$ for $y=0$.

The singular solution of Eq. (A.6) provides shearing forces

$$Q_x = -\frac{\partial}{\partial x}\left(D_x\frac{\partial^2 w}{\partial x^2} + H\frac{\partial^2 w}{\partial y^2}\right), \qquad (A.12a)$$
$$= -4\,C\left\{\bar{\gamma}\,(D_x + H\gamma^2)\left(\frac{1}{x+\gamma\,y} + \frac{1}{x-\gamma\,y}\right) + \gamma\,(D_x + H\bar{\gamma}^2)\left(\frac{1}{x+\bar{\gamma}\,y} + \frac{1}{x-\bar{\gamma}\,y}\right)\right\}$$

and

$$Q_y = -\frac{\partial}{\partial y}\left(D_y\frac{\partial^2 w}{\partial y^2} + H\frac{\partial^2 w}{\partial x^2}\right), \qquad (A.12b)$$
$$= -4\,C\left\{\bar{\gamma}\,(D_y\gamma^3 + H\gamma)\left(\frac{1}{x+\gamma\,y} - \frac{1}{x-\gamma\,y}\right) + \gamma\,(D_y\bar{\gamma}^3 + H\bar{\gamma})\left(\frac{1}{x+\bar{\gamma}\,y} - \frac{1}{x-\bar{\gamma}\,y}\right)\right\}.$$

The value of the constant C is now obtained from the fact that the concentrated load at the origin of co-ordinates is of unit intensity and so

$$\int_{-\pi}^{\pi}(x\,Q_x + y\,Q_y)\,d\theta = 1. \qquad (A.13)$$

In evaluating this integral it is noted that

$$\int\frac{x}{x+\gamma\,y}\,d\theta = \frac{1}{1+\gamma^2}[\theta + \gamma\log(x+\gamma\,y)],$$

$$\int\frac{y}{x+\gamma\,y}\,d\theta = \frac{1}{1+\gamma^2}[\gamma\,\theta - \log(x+\gamma\,y)]$$

and, in virtue of Eqs. (A.8),

$$\int_{-\pi}^{\pi}\frac{x}{x+\gamma\,y}\,d\theta = \int_{-\pi}^{\pi}\frac{x}{x-\gamma\,y}\,d\theta = \frac{2\,\pi}{1-i\,\gamma},$$

$$(A.14)$$

$$\int_{-\pi}^{\pi}\frac{x}{x+\bar{\gamma}\,y}\,d\theta = \int_{-\pi}^{\pi}\frac{x}{x-\bar{\gamma}\,y}\,d\theta = \frac{2\,\pi}{1+i\,\bar{\gamma}},$$

$$\int\limits_{-\pi}^{\pi} \frac{y}{x+\gamma y}\, d\theta = -\int\limits_{-\pi}^{\pi} \frac{y}{x-\gamma y}\, d\theta = -\frac{2\pi i}{1-i\gamma},$$

$$\int\limits_{-\pi}^{\pi} \frac{y}{x+\bar{\gamma} y}\, d\theta = -\int\limits_{-\pi}^{\pi} \frac{y}{x-\bar{\gamma} y}\, d\theta = \frac{2\pi i}{1+i\bar{\gamma}}. \tag{A.14}$$

Thus, when Eq. (A.12) is substituted into Eq. (A.13) and use made of Eqs. (A.15), (A.2) and (A.4), the value of C is found to be

$$C = \frac{-i\lambda^2}{16\pi\,(D_x D_y)^{1/2}\,\bar{\gamma}\,(\gamma^2 - \bar{\gamma}^2)}. \tag{A.15}$$

References

1. B. C. Best and R. West: Tests on a model of a continuous skewed slab supported on columns. Build. Sci., *1* (1965), 21.
2. W. Andrä and F. Leonhardt: Influence of the spacing of the bearings on bending moments and reactions in single-span skew bridges. Beton- und Stahlbetonbau, *55* (1960), 151. (Cement and Concrete Library Trans. Cj. 99.)
3. H. Rüsch and A. Hergenröder: Influence surfaces for moments in skew slabs. Selbstverlag MPA, München (1961). (Cement and Concrete Library Trans.)
4. L. S. D. Morley: Some variational principles in plate bending problems. Quart. J. Mech. Appl. Math. *19* (1966).
5. S. Timoshenko and S. Woinowsky-Krieger: Theory of plates and shells. McGraw-Hill, 2nd Ed. (1959).
6. Jean-Claude Leray: Calcul numérique des plaques fléchies. Arch. Mech. Stos. *17* (1965), 333.
7. Jean Leray: Calcul, par réflexions, des fonctions M-harmoniques dans une bande plane vérifiant aux bords M conditions différentielles, à coefficients constants. Arch. Mech. Stos. *16* (1964), 1041.
8. Jean Leray: Flexion de la bande homogène isotrope à bords libres et du rectangle à deux bords parallèles appuyés. Arch. Mech. Stos. *17* (1965), 3.
9. F. B. Hildebrand: Introduction to numerical analysis. McGraw-Hill (1956).
10. T. J. Jaramillo: Deflections and moments due to a concentrated load on a cantilever plate of infinite length. J. Appl. Mechs. *17* (1950), 67.
11. K. E. Robinson: The behaviour of simply supported skew bridge slabs under concentrated loads. Cement and Concrete Association Research Report No. 8 (1959).
12. J. Balas and A. Hanuska: Influence surfaces of skew plates. Vydavatel'stvo Slovenskej Akadémie Vied (1964).
13. M. Kurata and H. Okamura: Bending of a rectangular plate with two opposite free edges and other two simply supported edges having any clamped portion. Z. Angew. Math. Mech. *40* (1960), 310.
14. A. Mehmel und H. Weise: Modellstatische Untersuchung punktförmig gestützter schiefwinkliger Platten unter besonderer Berücksichtigung der elastischen Auflagernachgiebigkeit. Deutscher Ausschuß für Stahlbeton *161* (1964).

Summary

The theoretical analysis is given for the static behaviour of a thin flat isotropic plate which is rectangular in planform and is supported upon many diversely spaced columns and loaded by concentrated forces normal to its plane. The analysis employs the exact techniques which are associated with the classical theory of plate bending. A computer program has been prepared in conjunction with the analysis; it provides all the column reactions as well as the bending and twisting moments at any required station. Numerical examples are given along with extensive comparisons with the results of other authors and, in particular, with tests on the model of part of the elevated road system for the Cumberland Basin in Bristol.

An Appendix deals with the basic equations for orthotropic plates.

Résumé

On présente l'étude théorique du comportement statique d'une dalle mince plane isotrope, rectangulaire dans le plan, appuyée sur un grand nombre de piliers diversement espacés et soumise à des charges constituées par des forces concentrées normales à son plan. Pour le calcul, il est fait usage des méthodes rigoureuses qui correspondent à la théorie classique de la flexion des plaques. En liaison avec l'analyse, on a établi un programme de calcul électronique; celui-ci donne toutes les réactions des piliers ainsi que les moments fléchissants et les moments de torsion en tout point considéré. Des exemples numériques sont présentés et l'on procède à de nombreuses comparaisons avec les résultats obtenus par d'autres auteurs ainsi que, notamment, avec ceux des essais effectués sur le modèle d'une partie du complexe de routes surélevées prévu pour l'aménagement du Cumberland Basin de Bristol.

Les équations fondamentales des plaques orthotropes sont traitées en annexe.

Zusammenfassung

Die theoretische Analyse wird dargelegt für das statische Verhalten einer dünnen, flachen, isotropischen Rechteckplatte, welche auf vielen, in verschiedenen Abständen angeordneten Säulen liegt und von senkrechten Einzellasten beansprucht wird. Bei der Analyse werden die genauen Verfahren angewandt, die zur klassischen Biegetheorie der Platte gehören. Im Zusammenhang mit der Analyse ist ein Programm für den Elektronenrechner ausgearbeitet worden, das alle Säulenreaktionen sowie die Biege- und Drillmomente an jeder erforderlichen Stelle liefert. Es werden Zahlenbeispiele und umfangreiche Vergleiche mit den Ergebnissen anderer Verfasser und insbesondere Versuche am Modell eines Teils des Hochstraßensystems für das Cumberland Basin in Bristol gegeben.

Im Anhang sind die Grundgleichungen für orthotrope Platten behandelt.